MICA2 - Modelling Interaction between Cyclists and Automobiles 2

Public report

Project sponsored within the call for “Trafiksäkerhet och automatiserade fordon”.

Main author: Marco Dozza, Chalmers
Co-authors: Paloma Diaz Fernandez, Volvo Cars
Alexander Rasch, Chalmers
Prateek Thalya, Veoneer
Hanna Jeppsson, Autoliv
Francesco Costagliola, Volvo Cars
Yury Tarakanov, Viscando
Jesper Sandin, VTI
Magdalena Lindman, if
Date August 30th, 2023

Content

1. Summary

Every year, about 41000 **cyclists** die in road crashes and most of these **fatalities** happen in collisions with **motorized vehicles**. In Sweden, cyclists are the most-commonly-injured road user. **Overtaking manoeuvres**, where motorized vehicles circumvent cyclists, are particularly dangerous and offer a great opportunity for **active safety systems** to prevent crashes by warning the driver or by employing automated interventions. Further, in the overtaking scenario, **passive safety systems** to reduce injuries are still lacking.

While the FFI-project MICA (180401-191231) showed how driver models can help automated emergency braking systems become smarter and activate more effectively without compromising acceptability, the *MICA2 project addressed the safety of the **whole overtaking manoeuvre** by developing and testing prototypical **active and passive safety systems***.

Insurance claims databases and **crash databases** were analysed to determine the **crash scenarios** and crash-causation **mechanisms** for each overtaking phase. Several **behavioural models** were developed to address the whole overtaking manoeuvre. These models were not limited to the driver's **objective safety** but also considered the cyclist's perspective and the **perceived safety** of the different road-users. The models were used for the activation of **automated emergency braking** and **automated emergency steering**. In addition, **external airbags** and **expandable metal structures** were developed and tested in the project. The project also performed a **safety assessmen**t on the systems. For instance, the expandable metal structure from Autoliv reduced the AIS2+ head injury risk from 69% to 9%. In addition, an AEB system using MICA2 models, was able to avoid 20% of the crashes.

New **methodologies for data collection** were developed in the project, providing **unprecedented data** that was used to generate and verify the behavioural models as well as to **compare different test-environments**. Data was collected from **riding and driving simulators**. Further, **virtual reality** was employed in a **test-track** experiment to warrant the repeatability and safety of critical overtaking manoeuvres. Finally, by stitching several camera systems together, we collected unique **naturalistic data** showing how drivers overtake cyclists in the real world.

The results from MICA2 not only enabled new safety systems, but they also provided a fresh input for the development of experimental protocols in **Euro NCAP** and the promotion of a safe interaction between **automated vehicle** and cyclists.
Two **PhD students** graduated within MICA2. Further, the project produced more than 15 **journal papers** and **conference contributions**. Dissemination also included events in the **SAFER network** and a final even where the prototypical active and passive safety systems were **demonstrated** on the airfield in Vårgårda.

2. Sammanfattning på svenska

Varje år dör ca 41 000 cyklister i trafikolyckor och de flesta av dödsfallen inträffar vid kollisioner med motordrivna fordon. Av alla trafikantslag i Sverige, så är cyklister de som skadas oftast.
Omkörningar där motorfordon kör om cyklister kan vara mycket farliga. Här finns en stor potential att bidra till färre olyckor med nya aktiva säkerhetssystem - genom att varna föraren eller genom automatisk bromsning och/eller styrning. Det finns också stora möjligheter att minska personskadorna hos cyklister i omkörningskollisioner med hjälp av nya passiva säkerhetssystem.
FFI-projektet MICA (180401-191231) visade hur förarmodeller kan hjälpa automatiska bromssystem att bli smartare och aktiveras mer effektivt utan att kompromissa med föraracceptans. MICA2 har haft ett brett fokus på *hela* omkörningen då både aktiva och passiva säkerhetssystem har utvecklats och testats i projektet:

- Försäkringsdata och olycksdatabaser har analyserats för att identifiera **olycksscenarion och olycksmekanismer** för alla faser i omkörningen.
- Flera **beteendemodeller** har utvecklats för att hantera hela omkörningsmanövern vid simuleringar. Modellerna tar hänsyn till både förarens objektiva säkerhet, cyklistens perspektiv på situationen och den upplevda säkerheten för alla involverade trafikanter.
- Modellerna har använts för att utveckla och analysera **aktivering av automatisk bromsning och -styrning** i kritiska omkörningssituationer.
- **Externa krockkuddar och expanderbara metallstrukturer** för personbilar som kan lindra skadeutfallet hos cyklister har utvecklats och testats.
- En **effektanalys** av systemen har genomförts som visade att expanderbar metallstruktur på en bil kan minska risken för moderata/svåra huvudskador från 69% till 9%. Dessutom bedömdes att ett AEB-system med MICA2-modeller skulle kunna undvika 20% av omkörningsolyckorna helt.
- Nya **metoder för datainsamling** har utvecklats - som ger helt nya möjligheter att generera och verifiera beteendemodeller och att jämföra olika testmiljöer. Data har samlats in i både cykel- och körsimulatorer. Vidare har virtual realtity använts i ett experiment på provbana utan att äventyra deltagarnas säkerhet. Dessutom, genom att väva ihop indata från olika kamerasystem, har unika naturalistiska data samlats in med motorfordonsförare som kör om cyklister i verklig trafik.

Resultaten från MICA2 gör det möjligt att utveckla nya säkerhetssystem, ger ny input till utveckling av experimentella procedurer i Euro NCAP och främjar säker interaktion mellan automatiserade fordon och cyklister.
Två doktorander tog sin examen i MICA2 och projektet producerade mer än 15 tidskriftsartiklar och konferensbidrag.

För att sprida resultaten genomfördes olika evenemang i SAFER-nätverket samt en större demonstration på flygfältet i Vårgårda där både aktiva och passiva prototypsystem visades upp.

3. Background

3.1 Cyclist safety and overtaking

Transport modes are changing quickly, and more people are choosing sustainable alternatives to move and commute in the city. These alternatives, such as bicycles, electrical scooters or other micro-mobility vehicles, offer minimalistic protection, therefore their users are often referred to as vulnerable road users (VRU). Some cities protect VRU with separated lanes but in others, VRU share the road with motorized vehicles. This is also the case for inter-city roads, where it is common for VRU to share the road with vehicles by riding on the road shoulder. In Sweden, a total of 16,903 bicycle traffic crashes were reported in the Swedish Data Acquisition (STRADA) database during 2022 representing 36% of all traffic crashes registered in the system that year. 11,855 of these crashes were single-bicycle crashes with no other traffic-participant involved. Of the remaining 5,048, 2,450 were car-to-bicycle crashes, which resulted in 522 moderate-to-severe injury outcomes and 10 fatalities.

Most of the crashes between motorized vehicles and VRU occur at urban intersections, but the risk of a serious-to-fatal injury was observed to be significantly higher for crashes in same-direction scenarios than for crossing scenarios (Isaksson-Hellman I., 2017; Fredriksson R., 2014; IIHS, 2015; Wisch M., 2017). Researchers have previously conducted studies on same-direction crashes from different databases. Fredriksson et al. (2014) used the STRADA database for crashes where the severity score according to the Abbreviated Injury Scale (AIS) was AIS2+ (moderate-to-severe) and the Swedish Road administration fatal in-depth database. In this study, for the two scenarios that were found to be more frequent the motorized vehicle rear-ended a cyclist that was riding either straight or made a movement to the left. These two scenarios happened mostly in daylight conditions and on dry roads. Moreover, these two scenarios were the third and fourth most common scenarios for fatal car-vehicle crashes. The CATS project showed that same direction car-to-bicycle crashes investigated from databases from different European countries such as France, Germany, Italy, Netherlands, Sweden and United Kingdom account for 25% and 7% of the fatal and seriously injured cyclist (Uittenbogaard et al., 2016). Comparable results were found in studies performed with US data from NASS GES and FARS, where the most common situation for fatal crashes was cyclist traveling in line with traffic and vehicle moving straight (MacAlister A., 2015).

When cars and bicycles share the road, the drivers may overtake the cyclists, and if they misjudge distances, speeds, or times, a near-crash or a crash could occur. Therefore, is

important to support the driver with active safety systems to perform a safe overtaking manoeuvre.

3.2 Active safety systems

Active safety systems such as forward collision warning (FCW) and autonomous emergency braking (AEB) warn and intervene, respectively, as necessary to help drivers avoid collisions in critical situations. The main aim of an FCW is to notify the drivers of upcoming threats and potential collisions. The role of AEB is to brake automatically in critical situations to avoid a collision. Safety system include algorithms to estimate the threat and make decisions regarding their activation.

Previously reported algorithms for, threat assessment and decision making, range from methods based on simple vehicle kinematics to more sophisticated techniques which consider driver's actions as well. Methods based on simple vehicle kinematics, for example, may estimate time to collision (TTC) (B.-C. Chen et al., 2014), predict the minimum distance to the road-user ahead (Polychronopoulos et al., 2004), or calculate the deceleration required to stop and avoid the collision (Hillenbrand et al., 2006). Sophisticated methods may include: logic-based approaches which translate the requirements into logical sentences than specifying complex requirements (e.g., quantified differential dynamic logic (Loos et al., 2011)); set-based approaches, which formalize the requirements by specifying a set of acceptable or unacceptable system configurations (Kowshik et al., 2011); or probabilistic assessments, which assign probabilities to different events and road-user actions (Dahl et al., 2018).

Even though AEB systems are highly effective in avoiding collision, they are associated with some disadvantages, and emergency braking may not necessarily be the best course of action. Depending on the traffic situation, relative speed, availability of evasion space, and surface conditions, successful collision avoidance can be achieved by emergency steering. The distance needed to avoid the collision scales quadratically with the relative speed for braking and linearly for emergency steering. Work presented by Brännström et al. (Brännström et al., 2014) (Figure 1) highlight when steering to avoid collision is better than braking as a function of vehicle speed.

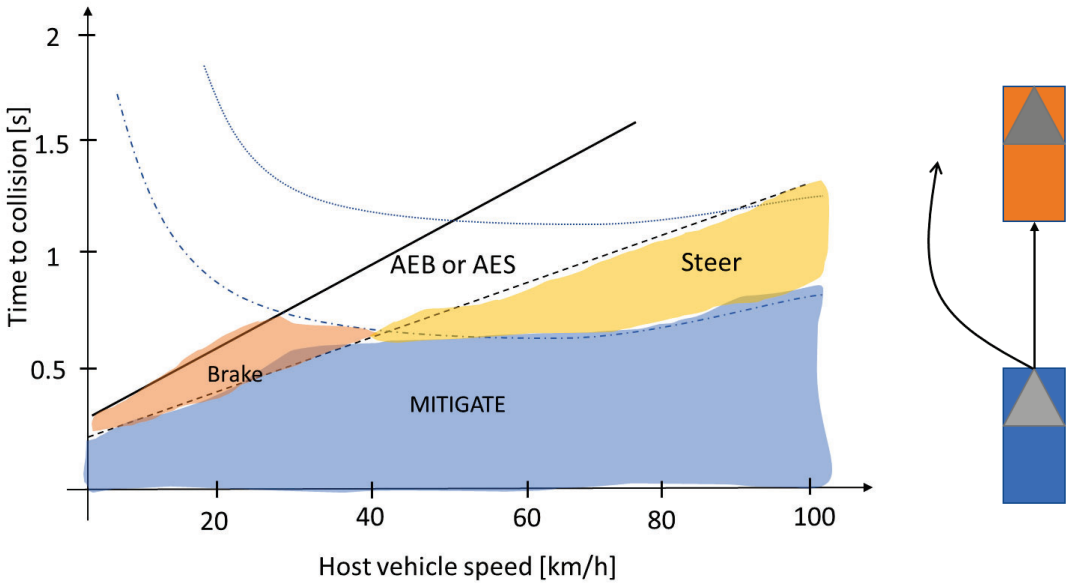

Figure 1: Relationship between vehicle host speed and time to collision and type of intervention required to avoid the collision. The figure is largely inspired by Brännström et al. (Brännström et al., 2014).

Collision avoidance strategy by steering can be carried out a) through Automatic Emergency Steering (AES) or b) through Emergency Steering Assist (ESA) (Seewald et al., 2015). Both ESA and AES perform a sudden evasive lane change via steering maneuver to avoid the collision. The main difference between the two types of systems is the way they are triggered. ESA works by providing additional steering torque on top of the driver steering torque when the risk is detected. However, unlike ESA, the AES can steer automatically when the detected risk of collision is over the designed threshold. The United Nations (UN) regulation No.79 (UNECE, 2021) details different types of steering systems fitted to the vehicles used on the road. The R79 covers regulations regarding advanced technologies with steering systems to improve the occupant's safety. The steering systems, where a driver is in primary control of the vehicle, are defined by R79 as "Advanced Driver Assistance Steering Systems". These systems vary in their functionality; to keep the vehicle on a set path (Lane-keeping), warn the driver of any deviation from the chosen lane (Lane Departure Warning), or keeping the driver from departing from the lane (Lane Departure Avoidance).

3.3 Behavioral models

A common challenge for active safety systems is the decision-making on whether and when to activate the system. If the system activates while the driver was in control of the situation, the driver might perceive the activation as a nuisance. After repeated exposure to false-positive activations, the driver might even switch the system off and thereby eliminate its safety benefits (Lübbe, 2015). Such *perceived* false positives differ from *technical* false positives where the system falsely activates due to sensor error. It can be

argued that a badly-functioning safety system can come at particularly high cost for the safety of the cyclist in situations where it is most needed.

Balancing false positives and true positives translates to the challenge of activating the system as early as possible to avoid collision with the cyclist, while, at the same time, activating as late as possible, to avoid annoying the driver. Models of driver behavior have been proposed as a possible solution to tackling this challenge, allowing the system to know when to act timely to allow complete collision avoidance (Brännström et al., 2013; Nosratinia et al., 2010; Sjöberg et al., 2010). Timely activations are particularly important for vulnerable road users like cyclists who may lose balance and fall as a consequence of even small disturbances (Schwab & Meijaard, 2013).

Driver models have been developed in research in various characteristics that can be differentiated by the modeling *level*, *objective*, *type*, and area of *application* (AbuAli & Abou-zeid, 2016). The level refers to the hierarchy of driving as proposed by Michon (1985), that can be *strategic*, *tactical*, or *operational*, depending on the time-scale of driver actions. The model's objective may be classified into *descriptive* or *predictive*, depending on whether the goal of the model is to allow inferences to describe how drivers behave, or to allow predicting specific quantities, possibly in real-time, that are usually intended to be used in active-safety systems. The (algorithmic) type of the model can range from purely *data-driven* to *cognitive-inspired* (AbuAli & Abou-zeid, 2016; Markkula et al., 2018). Application areas of driver models have been the development of active-safety systems (Sjöberg et al., 2010), automated-driving systems, as well as their evaluation in counterfactual simulations (Bärgman et al., 2017a).

Drivers' collision-avoidance behavior in interactions with other road users, such as cyclists, has long been investigated in research. Gibson and Crooks (1938) were the first to propose the theory of the *field of safe travel*, in which a driver's task is described to be navigating a vehicle through an environment with obstacles, while staying in a zone that is collision-free. Summala (2007) described this field of safe travel as a safety zone that a driver aims to stay within, while possibly compromising comfort when getting close to the boundaries of this zone. While the safety zone can be objectively defined by kinematics, the *comfort zone* may depend on subjective driver characteristics (M Ljung Aust & Engström, 2011). M Ljung Aust and Engström (2011) adapted these ideas into a framework that may be used for active-safety system development and evaluation, by, for instance, proposing that system activations should occur outside of the driver's comfort zone, to be perceived as useful (Mikael Ljung Aust & Dombrovski, 2013). Should the driver not react to e.g. a collision warning, an intervention system can still activate before leaving the safety zone.

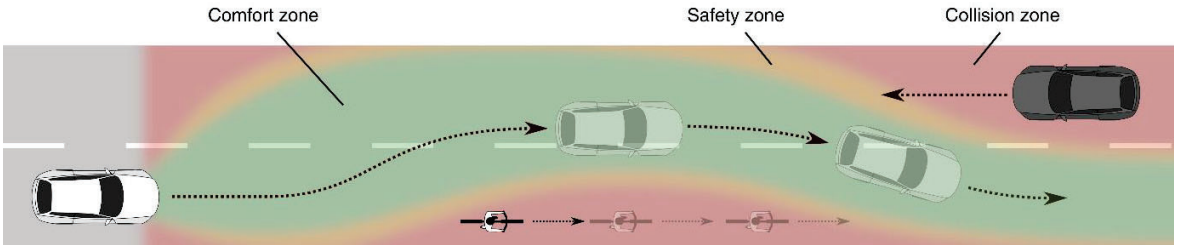

Figure 2: A driver's field of safe travel, with comfort zone, safety zone, and collision zone. Figure adopted from Rasch 2023.

Figure 2 shows how the field of safe travel, including the different zones could look like for a cyclist-overtaking maneuver. Driver behavior in such maneuvers has previously mainly been investigated through descriptive modelling to inform policymaking (e.g., legislation on passing distances or prohibition of overtaking) (Debnath et al., 2018; Lamb et al., 2020), or infrastructure design (e.g., design of cycle paths) (Bella & Silvestri, 2017; Shackel & Parkin, 2014).

In order to successfully complete an overtaking maneuver, a driver passes through several maneuvering *phases*. These phases are commonly defined as 1) *approaching*, 2) *steering-away*, 3) *passing*, and 4) *returning* phase (Dozza et al., 2016; Kovaceva et al., 2019). In the approaching phase, the driver recognizes the cyclist and possibly present oncoming traffic and needs to decide whether to overtake directly (flying maneuver) or first slow down and wait behind the cyclist (accelerative maneuver). The phase ends when the driver starts to steer out, which is the beginning of the steering-away phase, in which the driver aims to achieve a large enough lateral distance from the cyclist. In the next phase, the passing phase, the driver passes the cyclist while keeping sufficient lateral clearance. Once the driver has achieved sufficient longitudinal displacement from the cyclist, the driver can start the returning phase to get back to the original lane position.

Existing studies on cyclist-overtaking maneuvers have mainly focused on factors influencing lateral clearance, i.e., the lateral distance between car and cyclist at the moment of passing when car and cyclist are closest to each other (Rubie et al., 2020). This moment is critical as the combination of passing speed and clearance induce an aerodynamic drag on the cyclist that may destabilize the cyclist (Gromke & Ruck, 2021), or make the maneuver uncomfortable for the cyclist (Llorca et al., 2017; López et al., 2020). For instance, Dozza et al. (2016) showed in a field-test study that, in the presence of oncoming traffic, drivers kept lower clearances to the cyclist. In a simulator study, Bianchi Piccinini et al. (2018) showed that safety margins to the cyclist decreased when the time-to-collision (TTC) to the oncoming traffic was lower. Rasch et al. (2020) confirmed this finding based on test-track data and added that lateral clearance was decreased when the cyclist rode further inside the lane as opposed to the lane edge. Both factors were shown to affect the strategy decision of drivers, i.e., whether to overtake in a *flying* manner (without significant speed decrease) or an *accelerative* manner (slowing down behind the cyclist first and then re-accelerating to complete the overtake).

3.4 Safety benefit estimation

One way of estimating the safety benefit of either an active or passive safety system is to use injury risk curves. For active safety systems crash avoidance and speed reduction can be translated into injury and fatality reduction via the injury risk curves. The same principle can be used for passive safety system. To be able to estimate the effectiveness of for example an airbag the data has to be recalculated, and the injury risk curves re-drawn in a similar approach as Liers and Hannawald (2011). In this way, the new number of injuries will tell us what the effect could be if the cars were equipped with the new safety system.

To understand the effectiveness of active safety system in preventing fatalities when the system is still under development, assessments can be carried out virtually. These virtual assessments may involve counterfactual computer simulations on real-world crash or near-crash data (Bärgman et al., 2017b; Kovaceva et al., 2020; Sander, 2018) under various assumptions. The driver, vehicle, and environment are modelled to analyse the reduction in the number of crashes or fatalities in simulations with the modelled new system compared to those without it. The previous effectiveness studies have shown that AEBs are highly effective at mitigating intersection crashes (Sander, 2017) and rear-end crashes (Cicchino, 2017; Fildes et al., 2015) and also have shown to reduce cyclist fatalities (Rosén, 2013).

4. Purpose, research questions and method

The main novelty of this project is its **holistic approach to address a complex scenario** where multiple road users are interacting. In fact, this project combined different **crash scenarios** (rear-end, head-on, side swipes) as well as **active and passive safety systems**. (As opposed to only target one scenario and one system as it was done before.) In other words, the main purpose of the project was to develop and evaluate prototypical safety systems, leveraging road-user models and several data-types and testing facilities/tools available at the MICA2 partners.

The unique combination of competences and assets from a variety of partners (academia, OEMs, Tier1, small industries, insurance companies, and research institutes) employed in this project reflects the necessity of an **inter-disciplinary collaboration** across stakeholders to address in an original, holistic, and competent way the complex problem at hand. Specifically, the data and test facilities needed to develop the prototypical safety systems required not only the collaboration between industry, research institutes, and academia but also the support from an insurance company *if*, that provided **insurance claims** and a small company, Viscando that collected **unprecedented naturalistic data**.

The use of insurance data is novel and complemented the “more traditional” crash databases by providing a larger dataset and more information about the cyclist that is often missing in the crash databases because of underreporting. By combining these

datasets, the project could better address a basic research question in the project, colloquially: **"What goes wrong in cyclist overtaking?".** As for any solution, understanding the problem is the first step. By addressing this research question the project was able to get deeper insights into the problem and tailor solutions (i.e., models and systems) accordingly to go after the next question **"How can technology make overtaking safer?"**.

Because **data** was one of the most crucial assets of this project, we created a table to show how the data was shared/used across partners and work packages (WP). Table 1 shows how data types relate to the different efforts within our five work packages (WP) within this project.

Table 1: Main direct use of the data types by work package in MICA2. It is worth noticing that WP3 developed prototype safety systems and benefitted from data indirectly from WP1 and WP2, therefore WP3 does not show in this Table.

	Crash data	Insurance data	Experimental Data	Naturalistic data
WP1	Understand crash causation and injury mechanisms			
WP2			Develop driver models	Validate driver models
WP4	Define scenario for counterfactual analyses and run simulations to evaluate safety benefits			
WP5			Investigate the ecological validity of different test environments	

From a methodological perspective the main **innovations** from MICA2 include 1) the **Bayesian approach to road-user modelling**, 2) **the use of virtual reality on test track**, and 3) the test of novel tool such as **the riding simulator** at VTI and the **robot bike** at Chalmers. In the next chapter, WP2 expands on the road-user modelling and the use of these models as a **reference driver** for intelligent systems and **automated vehicles,** while WP5 addresses the test methodologies.

Prototypical passive and active safety systems were developed, evaluated, and demoed in the project. The active safety systems leverage the new driver models from MICA2. All systems were evaluated with a **safety benefit analysis** to show their potential impact in reducing crashes and injuries. In the next chapter, WP3 presents the systems and WP4 the safety benefit estimation. Figure 3, below, show the potential for different types of data to supply information for the safety benefit evaluation and contribute to a complete contingency table. This figure comes from the MICA2 proposal and guided the analysis in MICA2.

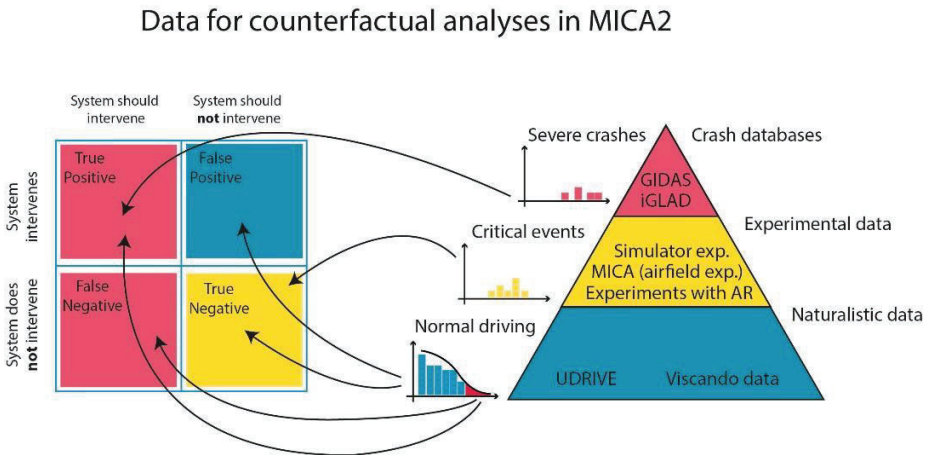

Figure 3: Relation between data types and contingency table for safety assessment using counterfactual simulations in the MICA2 project.

5. Objective

The aim of this project was to expand the work from MICA by improving safety for the whole overtaking manoeuvre and developing (and testing) prototypical active and passive safety systems.

To achieve this ambitious goal, this project devised several **behavioural models**, developed new **(virtual) tools and methodologies**, and investigated crash **causes and mechanisms** from **new data types**, such as insurance and site-based naturalistic data. Further, the project developed **prototypical active and passive safety systems** and estimated their **safety benefits**.

The results from this project contribute to:

1) improve **intelligent vehicle systems** such as FCW, AEB, and AES,
2) develop **passive safety systems** to prevent cyclist injuries in crashes,
3) create new tools and experimental methodologies based on **virtual reality** for system development and safety benefit estimation,
4) inform the design of test-scenarios for **Euro NCAP,**
5) help **autonomous vehicles** to safely interact with cyclists, and
6) determine how (**cooperative**) **applications** should support the interaction between cyclists and vehicles.

6. Results and deliverables

MICA2 comprised of 6 work-packages (WP0-WP5; see Figure 4 below). In this section, the results from each of the WP (with the obvious exception of WP0) are presented individually. At the end of each WP description, a short conclusion relates the results of the project in that specific WP to the objectives of the FFI-program while also explaining any deviation from the plan and the relation to the other WP.

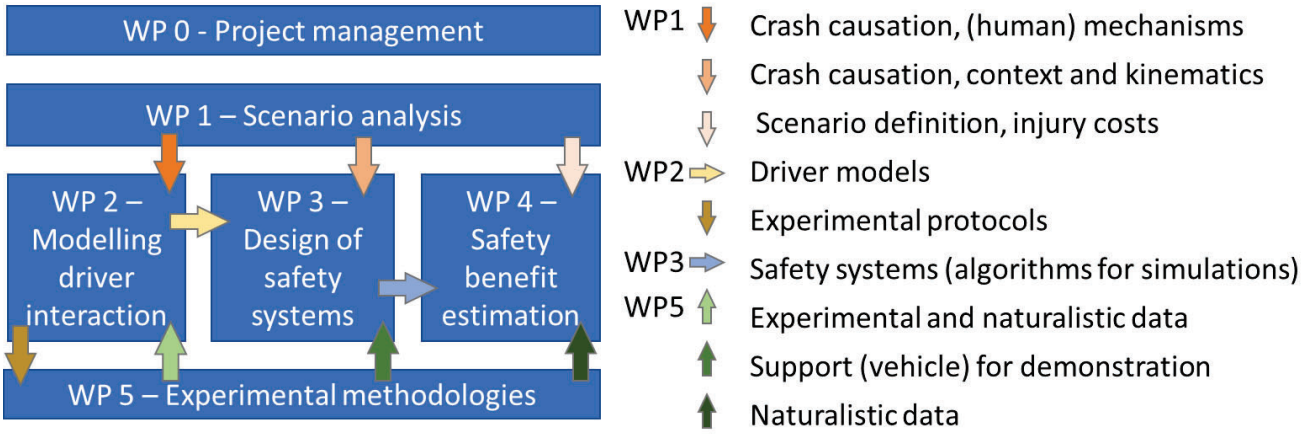

Figure 4: Work packages within the project and their main interactions.

6.1 WP1 – Results and deliverables

This WP described the crash scenarios for collisions between a passenger car and a bicycle in situations where an overtaking manoeuvre could take place. Only crashes where one bicycle and one passenger car that were traveling in the same direction and sharing the same road (i.e., without a physically separated bicycle lane) were considered. Impact configurations, pre-crash factors ,and injury outcomes fulfilling the described criteria pre-crash criteria were studied.

To obtain a relevant sample of crash-scenarios, the following four crash databases from different countries with both low and high crash severity were analysed:

- If_VRUC: car-to-bicycle crashes of vehicles insured by If P&C Insurance. This database covers crash severity from very minor to fatal. The database contains a description of the collision and in most cases, sketches, participants age and

gender, as well as information on environmental circumstances and location (Isaksson-Hellman, 2012). Cases from 2005 to 2018 were included in this study.

- V_CAD: car-to-bicycle crashes of Volvo cars vehicles insured by If P&C Insurance. Beyond the information available in If_VRUC map data of the crash scene, time-history-data (pre-crash paths in relation to velocities and surroundings), photos and damage evaluation according to SAE (Collision deformation Classification) were also available. Cases from 2005 to 2018 were included in this study (M. Lindman, 2015).
- GIDAS: includes traffic crashes with at least one injured person. These crashes occur in the German cities Dresden and Hanover and their surroundings, and there is a sampling weighting process in place that ensure that the data is representative in comparison with national statistics. The information is collected on-scene and almost 2,500 variables have been collected and reconstructed (GIDAS). Cases from all available years (1999-2020) were included.
- IGLAD: is an initiative initiated in 2010 by European car manufacturers for the harmonization of global in-depth traffic crash data to improve road and vehicle safety. The database contains crash data according to a standardized data scheme that strives to facilitate the comparison between datasets from different countries (IGLAD). For this study, cases for all available years (2007-2017) were included.

6.1.1 Crash scenarios

The total share of same-direction crashes could differ between databases depending on infrastructure designs in different countries and regions (as for example availability of bicycle lanes) or/and crash-severity in the database. However, we found similar patterns within same-direction crashes between the datasets which allowed for the classification of the crashes in three different crash-scenarios which are listed below:

1. Pure-same direction (CS1): collisions when there is no intention of turning into another road or changing lanes by either of the road users (66%).
2. Lateral movement of the bicycle (CS2): when the cyclist intends to turn into another road or change lane (18%).
3. Lateral movement of the car (CS3): when the car intends to turn into another road or change lane (17%).

The selection criteria applied to the four databases (If_VRUC, V_CAD, GIDAS, and IGLAD) resulted in 124, 31, 329, and 35 crashes, respectively. Figure 5 shows the distribution of car-to-bicycle same direction crashes in the three identified crash scenarios for the four datasets including the injury severity using the Maximum Abbreviated Injury Scale (MAIS).

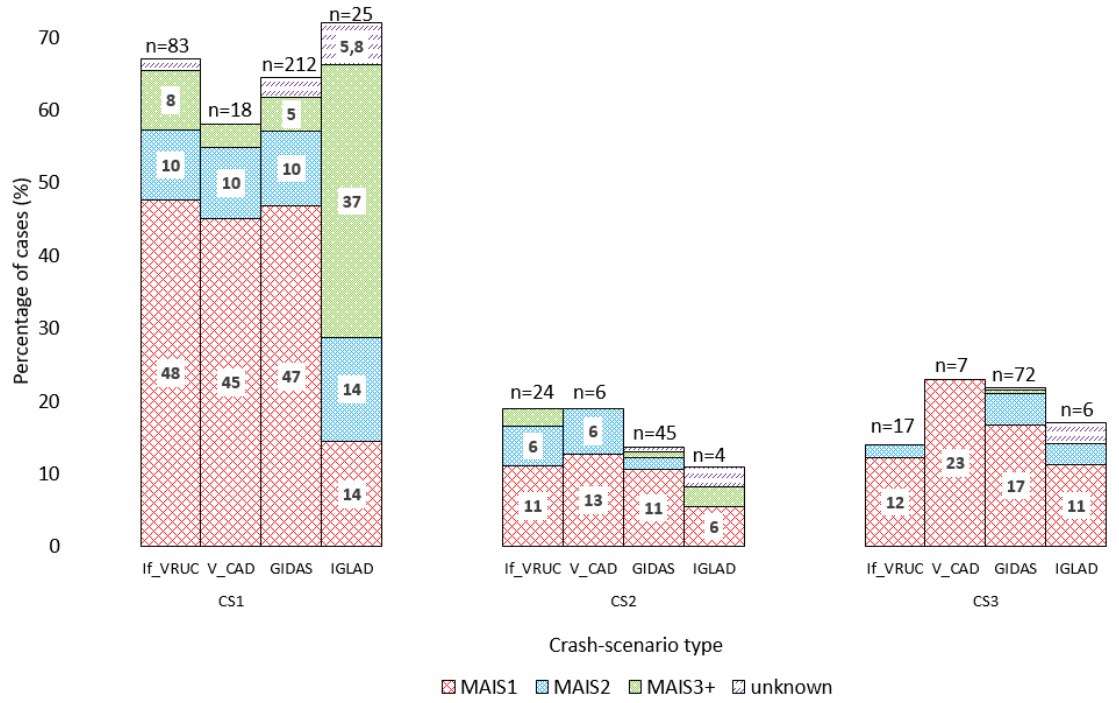

Figure 5: Distribution of crashes in percentage per dataset for the different same-direction car-to-bicycle crash scenarios (total number of crashes is shown on top of each bar). For each crash scenarios the MAIS shares are also shown providing an overview of the scenario severity per dataset. The numbers inside the bars indicate the percentages of cases with a specific injury level.

For all datasets, the most common crash scenario is CS1, with an average of 65%. The other two crash scenarios are approximately equally distributed. Most MAIS2+ injured cyclists are found in crash scenario 1. The injury severity distribution for the If_VRUC, V_CAD, and GIDAS datasets corresponds quite well for CS1, while the distribution for IGLAD includes a relatively higher share of MAIS3+ injured cyclists since that dataset for CS1 contained cases with higher injury severity. For CS2, the If_VRUC and V_CAD show a similar distribution trend, while GIDAS has a lower share of MAIS2+ in comparison. In IGLAD, only four cases were available in CS2, so no further comparison was made. In CS3, all four datasets are mainly comprised of cyclists with minor injuries (MAIS1). When comparing CS2 and CS3, an increase in injury severity is observed in CS2 (when the cyclist changes lane or turns) compared to CS3 (when the car is changing lane or turning).

CS1 was further grouped into the overtaking phases for V_CAD and If_VRUC. According to Dozza (M. Dozza, 2016), the overtaking manoeuvre can be divided into four phases; *approaching*, *steering away*, *passing*, and *returning*. In this work, the first two phases, *approaching* and *steering away*, were merged into one. Collisions in the different phases lead to different conflict situations. In the *approaching and steering* phase, the car hits the bicycle from behind, in the *passing* phase the car overtakes too closely, side-swiping the bicycle and in the *return* phase, the cut-in happens too early resulting in the bicycle rear-ending the car. The proportions of the different overtaking

phases in CS1 can be found in Table 2. Two cases could not be classified into one of the overtaking phases for V_CAD. The number of moderate (MAIS2) and serious-to-fatal (MAIS3+) injured cyclists was most frequent in the *approaching and steering* phase, followed by the *passing* phase. The *returning* phase mostly caused slight injuries to the cyclists.

Table 2: Proportion for the different overtaking phases for If_VRUC and V_CAD databases.

Overtaking phase	If_VRUC (%)	V_CAD (%)
Approaching and steering	42	28
Passing	41	39
Returning	17	22

Pre-crash factors were also studied for the four datasets, and it was observed that crashes occurred more commonly in spring and summer, during daylight, between 7 and 19 o'clock, on dry roads, and without precipitation. The most common road type was found to be an urban road or a road segment in a rural road that is not in a crossing. The posted speed limit was found to be between 40-60 km/h in more than half of the cases. Most cyclists were male and between 15-64 years.

Some of the pre-crash factors such as type of road, light and road conditions, posted speed limit, initial and collision speeds, were studied in more detail for the different crash scenarios. For those, the distributions for all cases were compared with two subsets, one with MAIS0-1 and one with MAIS2+.The distribution of the type of road showed that, while CS1 and CS2 contained crashes in both urban and rural areas, CS3 contained only crashes in urban areas. In agreement with this, the distributions of the posted speed limit per crash scenario showed that the proportion of crashes on roads with higher posted speed limits was larger in CS1 and CS2 compared with CS3. It was observed that the number of cases that happened on rural roads increased its share for the MAIS2+ subset in all datasets, especially for CS1, which were found to be more common on roads with higher posted speed limits. The distributions per crash scenario for the light conditions for the two injury subsets showed an increase in the number of cases in darkness and dawn/dusk conditions when looking at the sample with a higher injury severity, MAIS2+. An increase in the number of crashes that happened in wet road surface conditions was also found in the datasets from If_VRUC and GIDAS. The If_VRUC dataset presented also a similar number of cases on roads with snow/ice than on wet roads. The initial speed of the car was found to be below 40 km/h in most of the cases, but a significant number of crashes had higher initial speeds. Collision speeds were also found to be more frequently below 40 km/h, but there was also a non-negligible number of crashes with higher speeds. When studying speed parameters for the different scenarios, it was observed that crash scenario 3 contained only cases where the initial and collision speeds were below 60 km/h, while the other two crash scenarios contained a more diverse distribution of values.

The contributing factors that lead to the crashes were found in the crash descriptions narratives. The most common contributing factors found are listed as following: insufficient safety distance when performing an overtaking manoeuvre, overtaking performed despite an unclear traffic situation (unknown presence of oncoming vehicles, cyclist turning left, the driver intends to turn right assuming that the cyclist has the same intention), mistakes made when returning to the lane (car returned very quickly for example because of oncoming vehicle, car had a trailer attached and underestimated its length, etc.), driver blinded by the sun, misunderstanding of each other's intentions at a crossing and inattention. These can be compared with other crashes scenarios such as those for crashes occurring on intersections where lack of visibility and obstructions are found to be the main contributing factors while in same-direction crashes visibility is not usually a problem. More analysis results can be found in the publication (P.Diaz Fernandez, 2022).

6.1.2 Injury curves

In D1.2 "Injury risk curves for lateral car to cyclist impacts" the injury risk was assessed by Injury Risk Curves (IRC). IRC evaluate the risk of sustaining an injury in a crash as a function of speed. The cyclist IRC calculated in this study depends only on closing speed. In Table 3, the results from the logistic regression for Fatal, MAIS3+ and MAIS2+ injury severity is shown. The injury risk curves with 95% confidence intervals and injured and uninjured cyclists (grey stars jittered around 1 on y-axis for injured, around 0 for uninjured cyclist) are shown in Figure 6a-6c.

Table 3: Result from logistic regression, p-value, for fatal, MAIS3+ and MAIS2+ in same direction car-to-bicycle crashes.

		Best estimate	**Lower limit**	**Upper limit**	**p-value**
Fatal	b_0	-6.645	-8.93	-4.36	<0.001
	b_1	0.0846	0.036	0.133	
MAIS3+	b_0	-4.708	-5.863	-3.553	<0.001
	b_1	0.071	0.039	0.102	
MAIS2+	b_0	-1.898	-2.405	-1.391	<0.001
	b_1	0.039	0.020	0.059	

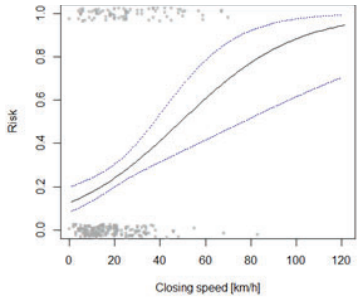

Figure 6a, Injury risk curves for cyclists sustaining MAIS2+ injuries with 95% confidence interval in same direction car-to-bicycle crashes

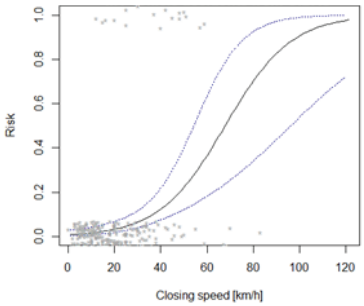

Figure 6b, Injury risk curves for cyclists sustaining MAIS3+ injuries with 95% confidence interval in same direction car-to-bicycle crashes

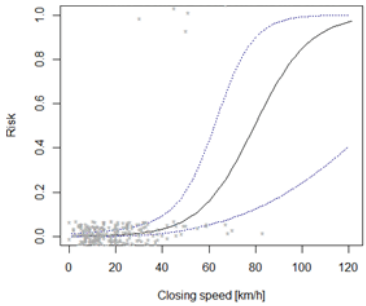

Figure 6c, Injury risk curves for cyclists sustaining fatal injuries with 95% confidence interval in same direction car-to-bicycle crashes

From the risk curves the injury risk at a certain speed can be determined. The speed limit in many urban areas is 50 km/h, which gives a 50% risk of an MAIS2+ injury, just above 20% of an MAIS3+ injury and below 10% risk of a fatal injury according to the IRC.

In conclusion, WP1 described crash scenarios (D1.1; VCC) and created injury curves (D1.2; Autoliv) for the longitudinal interaction between motorized vehicles and cyclists. These results were used within the project to motivate several decisions and, in particular, for the design of the experiments in WP5 and the safety evaluation in WP4. By explaining how crashes distribute among overtaking phases, the results from this WP help appreciate the potential safety benefits that different safety systems (supporting the driver in different overtaking phases) may have. In other words, this WP contributed to the overall goals of this project and of the FFI programme by increasing our knowledge about the safety problem in overtaking manoeuvres, pointing out which factors to include in our experimental protocol and in which situations the benefit from active and passive safety are highest.

6.2 WP2 – Results and deliverables

This WP has developed descriptive and predictive models of driver and cyclist behaviour, considering both objective and subjective, perceived safety. The models were developed based on the test-track (TT) dataset from MICA (Rasch et al., 2020), and the datasets collected in WP5. Furthermore, this work package developed the experimental protocols for the data collections in WP5, in close collaboration with WP5 and informed by WP1.

The following milestones and deliverables were addressed in WP2:

- M2.1 Protocol for cycling simulator experiment
- M2.2 Protocol for driving simulator experiment
- M2.3 Protocol for AR experiment
- D2.1 Expanded driver models covering all phases using MICA data

- D2.2 Expanded model covering critical situation using augmented reality and simulators data
- D.2.3 Driver model validation on naturalistic data

During the project, all milestones and deliverables were completed. The deliverables were slightly different than what was planned in the beginning mainly as a consequence of the augmented reality system that did not perform good enough to be used for data collection. As a consequence the work focused on virtual reality (this point will be further discussed in WP5).

The experimental protocols developed in WP2 included the ones for 1) the cycling-simulator experiment at VTI (M2.1), 2) the driving-simulator experiment at VTI (M2.2), and 3) the DVIL experiment with VCC at Veoneer (M2.3).

6.2.1 Cycling simulator experiment

For the cycling-simulator experiment (Figure 7), which was based on a replication of a real-world intersection scenario between a cyclist and a motorized vehicle, nine trials were designed by varying the variables 1) time-to-arrival (TTA) of the cyclist, 2) field-of-view (FOV) distance, and by adding a surprise event at the end. TTA was defined as the time that it would take the cyclist to reach the intersection point between the vehicle's and the cyclist's predicted paths. FOV distance was controlling the position of a visual obstruction to the cyclist. The results from this experiment have been presented at ICSC in 2022 (Mohammadi et al., 2022) and a follow up study will be presented at ICSC in 2023 (Mohammadi et al., 2023). The analysis was performed in collaboration with the SHAPE-IT project by one of Chalmers PhD students, Ali Mohammadi. The models developed by Ali show which factors play a role in the interaction between cyclists and drivers, confirming that kinematics cues play the largest role. Most importantly, this experiment helped us understanding the current limitation on bicycle simulators.

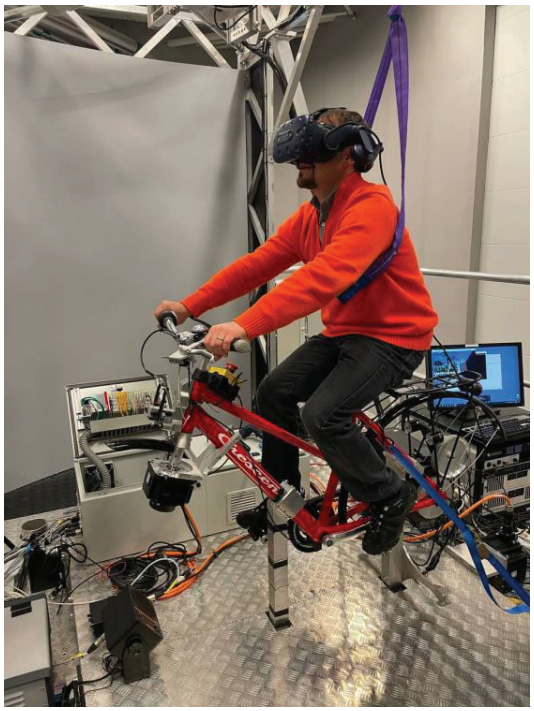

Figure 7: Riding simulator at VTI.

6.2.2 Driving simulator experiment

The experimental protocol for the driving-simulator experiment included overtaking scenarios of cyclists on a continuous, artificial two-lane rural road. The road was continuous to keep participants maximally emersed in the driving task and avoid unnecessary braking and accelerating, which could have induced nausea. Two roads were designed, consisting of longer straight-road stretches connected by curve elements: one road started with a speed limit of 50 km/h and, after four overtakes continued at 70 km/h, and the other road for the opposite order. Participants completed a total of eleven overtaking manoeuvres, resulting from variations of the speed limit, the TTC to an oncoming vehicle, the presence/absence of guard rails (Figure 8), and with a last, critical scenario. TTC was varied between NA (no oncoming), 9 s, 6 s, and 3 s, measured at the moment when the ego vehicle reached 2 s TTC behind the cyclist in accordance to (Rasch et al., 2020). In the critical scenario, drivers met an oncoming vehicle that was controlled to meet the driver at a TTC of 6 s, and then started to accelerate. The first event was always without oncoming vehicle. Then, randomizations were performed for the variable TTC (9 s, 6 s, and 3 s), within each speed limit, resulting in six events. The eighth event was again without oncoming vehicle, followed by two overtakes with guard rails present (with TTC at 6 s and 9 s), followed by the last, critical event (without guard rails).

a) without guard rails b) with guard rails

Figure 8: Driving-simulator scenario; overtaking a cyclist without guard rails (panel a), and with guard rails (panel b).

6.2.3 Test-track experiment

The experimental protocol for the DVIL experiment was set up to resemble the scenario from the driving-simulator experiment as well as the test-track experiment from MICA, as closely as possible (Figure 9). Due to the limitation of the physical environment (Vårgårda airfield), a continuous road was not feasible. Therefore, a similar set up as in MICA was chosen: a participant drove the ego vehicle on a straight road stretch from one end of the airfield toward the other end. The road environment was adopted from the driving-simulator experiment. The protocol consisted of a total of twelve trials for each participant, resulting from variations of the factors 1) speed limit (50 km/h and 70 km/h), 2) TTC to oncoming vehicle (NA, 9 s, and 6 s), and the cyclist lane position (0% vs 50% lateral overlap with the ego vehicle), in accordance to (Rasch et al., 2020).

Figure 9: Snapshot from the DVIL environment.

6.2.4 Behavioural models

The driver models from MICA were expanded by addressing all phases of the overtaking manoeuvre in greater detail (D2.1), with an emphasis on the later phases. Furthermore, the models expanded the scope of driver models by capturing the *cyclist* perspective, addressing the perceived safety of both road users. Naturalistic data collected in WP5 were used to validate the models (D2.3).

For the passing phase, models of drivers' and cyclists' perceived safety were developed. Based on cyclist data provided by the Highway Engineering Research Group of the Technical University of Valencia (Moll et al., 2021), and driver data from MICA, Bayesian ordered logistic regression models were fitted to express perceived safety in response to variables strategy choice (flying vs accelerative), lateral clearance, passing speed, oncoming presence, and TTC to oncoming. Thanks to the Bayesian approach, the models can predict a probability mass distribution of credible perceived-safety scores on a Likert scale (Bürkner & Vuorre, 2019). Results for the fitted parameters revealed that neither drivers' nor cyclists' safety perceptions were clearly affected by strategy choice, but cyclists perceived higher risk in overtaking manoeuvres performed at low clearance and high speed, while drivers felt more discomfort in the proximity of an oncoming vehicle. These models could enable driver-coaching systems that inform the driver of the cyclist's perception, for instance, after each performed overtake. Furthermore, automated-driving systems may use the model's predictions to generate a "fair" overtaking path that is maximally comfortable for all road users. This study was published in (Rasch et al., 2022).

Furthermore, for the passing moment, models based on Viscando's naturalistic data were developed to show the effect of visibility in terms of the sight distance available to the driver. A Bayesian multivariate model was fitted on the overtaking events to jointly model both lateral clearance and speed since a correlation between these metrics was assumed (Figure 10). The model's input variables included the sight distance, the presence and distance of an oncoming vehicle, as well as the width of the ego vehicle and the speed of the cyclist. The results for the parameter distributions indicated that the presence of an oncoming vehicle had a strong effect on both clearance and speed, reducing both of them but clearance with a stronger effect. Sight distance affected lateral clearance in a similar way as the distance to an oncoming vehicle, resulting in lower clearances for lower distances. The model could inform infrastructure design and policymaking on how to adjust for areas with limited visibilities to ensure cyclist safety. This study was accepted for publication in the Journal of Safety Research (Rasch et al., in press).

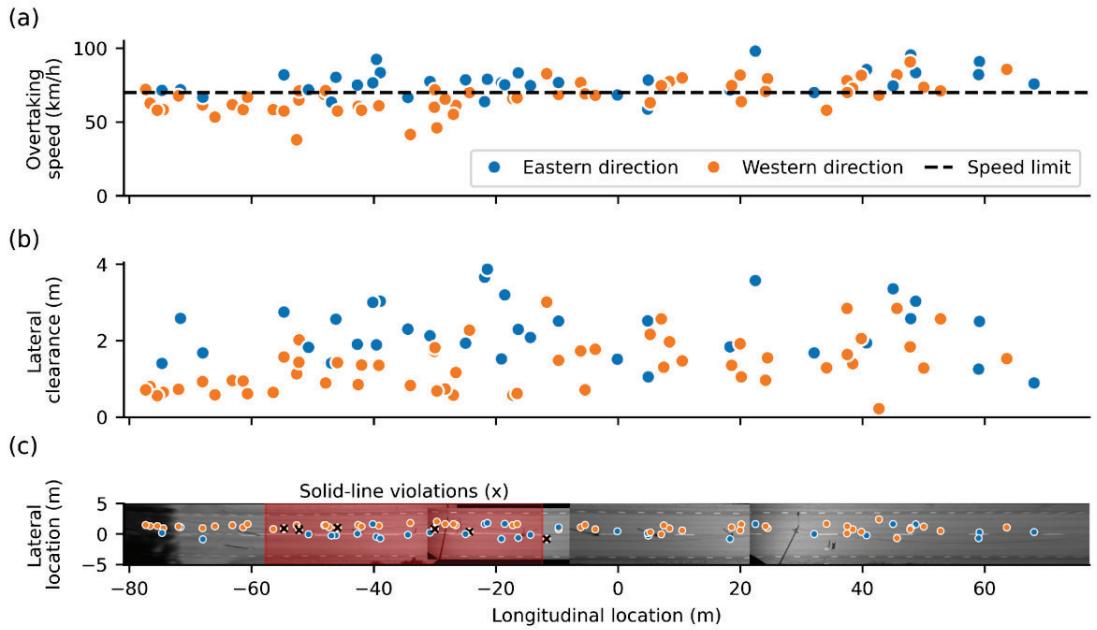

Figure 10: Data used for analyses of the effect of available sight distance on lateral clearance and overtaking speed when passing cyclists. At the western end of the road (left), the available sight distance was lower than toward the eastern end (right).

For the passing and returning phases, a model of driver behavior was developed based on the test-track data from MICA, and, for validation purposes, also on the naturalistic data collected by Viscando in WP5. The model expresses the timing of the driver to initiate the returning phase, after having initiated the passing phase. For this purpose, a Bayesian survival model was developed that utilized all time-series data from the passing phase in a discrete-time representation (Singer & Willett, 2003). The predictive performance of the model in terms of *discrimination* (distinguishing the two possible events, *before* return onset vs *at* return onset) and *calibration* (predicted probabilities match with observed) was assessed in a cross-validation scheme. Both models performed reasonably well in the cross-validation. Results for the parameters showed that drivers accelerated their passing phase when an oncoming vehicle was present and close. The same basic model structure was fitted on each dataset and revealed parameters in similar directions, contributing to the cumulative evidence of our findings. The model could be used to improve active-safety systems such as blind-spot detection systems that warn the driver to prevent a side-swipe collision, or forward-collision warning systems to prevent a head-on collision with oncoming traffic. By using the model to predict when drivers normally return, the system could identify a mismatch with the driver's current actions and adjust the system-activation timing accordingly.

The number of critical maneuvers available in the driving-simulator and DVIL datasets was deemed too low for statistical analyses (D2.2), as a result of a brief analysis of both objective and perceived safety measures. Lateral clearance was below 1.5 m (the most common regulation in EU) in only 36 events (5.37% of all events, 16 in the driving simulator and 20 in DVIL), and below 1.0 m (lowest regulation) in only three events

(0.45%, two in driving simulator and one in DVIL), as shown in Figure 11. Cyclist perceived risk was predicted with the previously developed model (Rasch et al., 2022), and greater than medium risk only in only seven events (three in SIM, four in DVIL). Driver discomfort was never predicted to be greater than level three (on a scale from one, i.e., minimum discomfort, to seven, i.e., maximum discomfort).

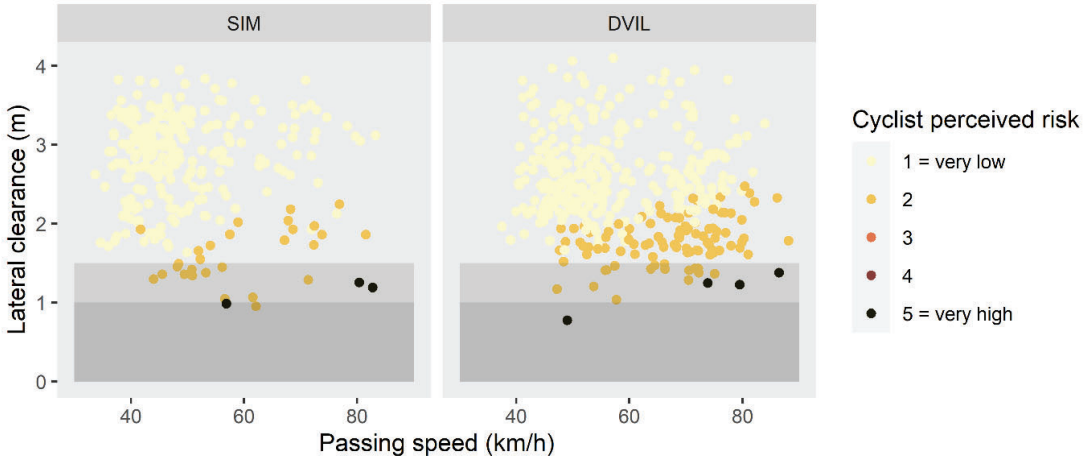

Figure 11: Lateral clearance over passing speed for driving-simulator (SIM) and driver-vehicle-in-the-loop (DVIL) datasets. The gray shaded areas mark common regulations for minimum lateral clearance of 1 m and 1.5 m. The color indicates the predicted cyclist perceived safety, predicted by the model from Rasch et al. (2022).

Instead, a different analysis was performed on both datasets to investigate the effect of approaching speed on drivers' strategy choice and safety metrics like lateral clearance. Preliminary results revealed that in events with oncoming traffic present, drivers preferred the flying strategy at higher approaching speeds (70 vs 50 km/h instructed speed). Lateral clearance, on the other hand, did not increase accordingly. Lateral clearance did increase as a consequence of larger time gaps to oncoming traffic, which also resulted in more flying maneuvers, compared to shorter time gaps. The results will be presented at the ICTCT 2023 conference (Rasch et al., 2023).

In conclusion, WP2, informed by WP1, contributed to several experiments performed in WP5 by devising their experimental protocol. WP2 also performed analysis from the data collected from these experiments as well as data from MICA1 and naturalistic data from Viscando collected in WP5. WP2 delivered several scientific contributions (journal and conference papers) that described several behavioural models covering all phases of the overtaking manoeuvres. These models served as an input to WP3 for the development of prototypical safety systems. It is worth noting that WP2 also compared the test environments in WP5 therefore contributing also several methodological results.

In other words, the main contribution of this WP to the project and to the FFI program goals was the mathematical description (i.e., model) of road-user behaviour in all phases of an overtaking manoeuvre. Such models may help intelligent systems warning a driver (or automatically intervening) before a crash with a cyclist may happen (see WP3). These models can also explain to automated vehicles how a reference driver may safely

overtake a cyclist. It is worth noting that the models also predict what would feel safe from a cyclist perspective creating the opportunity for an automated vehicles to maximize safety for all road users (including potential oncoming traffic) and not only for the driver of the overtaking vehicle. Finally, because WP2 used different data to develop, verify, and validate models, it also compared the different test environments in MICA2. The results from such comparisons are further discussed in WP5.

6.3 WP3 – Results and deliverables

The main aim of this work package was to design new prototypical safety systems. The design of safety system was spilt into active and passive safety systems. In active safety system development, a combined automated emergency braking (AEB) and automated emergency steering (AES) model was developed to address the crash risks during the overtaking of a cyclist. From the passive safety system development, a new B-pillar concept was developed in finite element simulation and a prototype external protection system was also developed. The system designed were demoed during the final event of the project.

The deliverable reported during WP3 are summarized below. In deliverable D3.1 (*Possible opportunities to combine AES with AEB to support the different phases of the overtaking)* a review was carried out to understand the difference between different collision avoidance systems in terms of braking and steering; what are the legal limitations in relation to steering systems; type of steering system available in the market.

6.3.1 Review of UN ECE R79 – Steering functions

The United Nations (UN) regulation No.79 (UNECE, 2021; will be referred to as R79 from now on) details different types of steering systems fitted to the vehicles used on the road. The R79 covers regulations regarding advanced technologies with steering systems to improve the occupant's safety. The steering systems, where a driver is in primary control of the vehicle, are defined by R79 as "Advanced Driver Assistance Steering Systems". These systems vary in their functionality; to keep the vehicle on a set path (Lane-keeping), warn the driver of any deviation from the chosen lane (Lane Departure Warning), or mitigate the driver from departure from their lane (Lane Departure Avoidance)

The different types of steering systems defined in R79,

1. *Autonomous Steering System* - a system that causes the vehicle to follow a defined path or to alter its path where the driver will not necessarily be in primary control of the vehicle.

2. *Advanced Driver Assistance Steering System* - a system that aids the driver in steering the vehicle in which the driver always remains primary control of the vehicle. The function is further classified into:

a. *Automatically commanded steering function (ACSF)* - a function where the steering system can generate control action to assist the driver.

b. *ACSF of Category A* - a function that operates at a speed less than 10km/h to assist the driver, e.g., low speed or parking maneuvering.

c. *ACSF of Category B1* - a function that assists the driver in keeping the vehicle within the chosen lane.

d. *ACSF of Category B2* - a function activated by the driver and keeps the vehicle within its lane for extended periods without further driver confirmation.

e. *ACSF of Category C* - a function activated by the driver and performs a single lateral maneuver (e.g., lane change) when commanded by the driver.

f. *ACSF of Category D* - a function activated by the driver, which can indicate the possibility of a single lateral maneuver (e.g., lane change) but performed following confirmation by the driver.

3. *Corrective Steering Function (CSF)* - a control function observes a change to the steering angle of one or more wheels in order: a) to compensate for a sudden, unexpected change in the side force of the vehicle, or b) to improve the vehicle stability, or to correct lane departure.

4. *Emergency Steering Function (ESF)* - a control function that can automatically detect a potential collision and automatically activate the vehicle steering system for a limited duration to steer the vehicle to avoid or mitigate a collision,

    a. With another vehicle driving
        i. in an adjacent lane:
        ii. Drifting towards the path of the subject vehicle and/or.
        iii. Into which path the subject vehicle is drifting and/or.
        iv. Into which lane the driver initiates a lane change maneuver.

    b. With an obstacle obstructing the path of the subject vehicle or when the obstruction of the subject vehicle's path is deemed imminent.

6.3.2 Emergency Steering Assist (ESA) – systems on the market

Several production vehicles employ the ESA function to mitigate the collision with the obstacle in ego vehicles path. ESA functions are categorized as Automatically commanded steering functions under the categorization of UN regulation. The primary principle for activating the ESA is to avoid contact with another vehicle if braking is considered insufficient. ESA utilizes data fusion based on a vision and a radar sensor that

detect the situation in front of the vehicle. If the driver initiates emergency steering when a collision with an object is imminent, ESA generates an additional steering torque that assists the driver (Seewald et al., 2015). Examples of ESA systems on the market,

a) The EAS function by Volvo called "City safety with steering assist" (Cars, n.d.) helps the driver to take an evasive steering action if it is determined that collision cannot be avoided by braking alone. City Safety triggers steering assistance when the driver begins an evasive action to try to avoid a collision but only if the driver's steering actions are not sufficient to avoid the collision.

b) Evasive steering assist by Ford (Ford, n.d.) works in connection to the AEB system which detects the stopped vehicle in front of the ego vehicle using combined camera and radar technology. The system provides additional steering support when drivers' steering is not enough to avoid the collision.

c) Pre-collision system with active steering assist by Lexus (Lexus, n.d.) is activated when braking is not enough to avoid the collision, thus triggering the active steering assist in changing the course of the ego vehicle.

As part of the deliverable, a review of relevant literature was carried out to understand research related to steering functions. The literature found was broadly classified into three categories a) implementations of steering function, b) decoupling driver from the steering function and c) combined emergency braking and steering.

6.3.3 Implementations of steering function

When it comes to implementing a steering function to avoid the collision with an object in front of the ego vehicle, previous work has been focused on the Steering system performing a single lane-change maneuver and keeping the vehicle stable during the maneuver. The instability of the vehicle during the steering maneuver arises due to characteristics of tyre forces becoming nonlinear and making it difficult to stabilize the vehicle in emergency conditions. The stability of the vehicle can be improved by optimal control strategy; for example, work by He et al. (He et al., 2019) proposed a steering control strategy based on hierarchical control to achieve improved collision avoidance and stability of the vehicle. Or using 5th order polynomial and nonlinear vehicle lateral controller proposed by Seewald et al. (Keller et al., 2014; Seewald et al., 2015) for a semiautonomous vehicle.

When it comes to implementing the AES systems, different approaches have been taken to, such as using Reinforcement Learning (Yoshimura et al., 2020), where the controller is trained using a deep neural network which calculates the optimal trajectory and the system is activated based on time to the collision to the object to avoid the collision. Similarly, work by Adelberger & Del Re (Adelberger & Re, 2020) proposed a two-layer approach to provide an optimal escape trajectory to perform safe steering. Other approaches to implementing an emergency steering system include an improved path planning algorithm which uses map data to generate an optimal path for a short distance

ahead to perform safe steering (Jafari et al., 2017). Similarly, Chen et al. (M. Chen et al., 2019) proposed a required safe distance-based algorithm to avoid rear-end collisions where safe distances were calculated based on Monte Carlo simulation for different scenarios. An algorithm proposed by Hong et al. (Hong et al., 2013) uses the driver intention index, where the index is generated by driver intention to perform a lane change maneuver.

6.3.4 Ways to decouple to the driver when ESF is active

Decoupling the driver also invokes issues that are commonly associated with performance breakdowns in human-machine systems. For example, decoupling the driver while providing torque feedback may mislead the driver to believe that they are in control of the vehicle. Moreover, highly automated driving systems such as decoupled driving may reduce driver vigilance and situation awareness due to a reduced involvement of the driver in the driving task (Chen et al., 2019; Hong et al., 2013; Euro NCAP, 2020; Vassilis et al., 2015). In particular, drivers who become aware that they have little or no control over the vehicle may fail to intervene if automation fails to activate (Jafari et al., 2017; Clarke et al., 1999). On the other hand, drivers unaware of their level of control authority might be surprised or confused by an automation-initiated maneuver (or lack thereof) and left wondering why automation behaved in a certain way (Heesen, 2014).

6.3.5 Combing emergency braking with steering

Results from MICA1 showed that FCW and AEB system may not be able to avoid all the crashes. The missed activation of the proposed driver model-based system shows that there is a room for complimenting MICA1 systems with steering functions. The remaining crashes failed to be addressed by can be used to motivate implementing ESS function to provide steering to move the ego vehicle away from the bicycle. ESS may not be useful or need to be reconfigured to address different collision risk in the other phases of overtaking (Rasch et al., 2020).

However, Shimizu et al. (Masayuki Shimizu; et al., 2008) showed that 37.9% of drivers did not take any avoidance manoeuvres when encountering the approaching an obstacle. This highlights that an inattentive driver cannot be guaranteed to perform late steering to avoid a collision. Thus, rather than ESS, AES can be implemented to automatically detect the risk of collision and activated to mitigate or avoid the collision.

However, there is a lack of research on implementing steering function for the overtaking scenario. Therefore, based on the literature on lateral control functions, a parameter list is defined as part of D3.2 to develop an emergency steering function specifically for the overtaking scenario to address the rear-end crashes with the bike. The effectiveness of the function is dependent on a) lateral acceleration levels, b) defined lateral offset, c) type of steering (S or J steering), and d) presence of free space for function activation.

6.3.6 Proposed expandable B-Pillar concept design for bicyclist protection

In delivery D3.3 “Proposed expandable B-Pillar concept design for bicyclist protection” a finite element model of an injury-reducing, expandable, metal structure was created and mounted on the side of a vehicle. The expandable metal structure is folded during normal driving of the vehicle and will expand by means of a gas generator in case of an impact with a bicyclist. The simulation was carried out in LS-Dyna using the SAFER Human Body Model (Pipkorn et al., 2023) (Figure 12a). The bicycle was impacting the vehicle in 20 km/h varying the impact angle between, 60°, 90° and 150° (Figure 12b). The vehicle stood still in all simulations except in one configuration where it was moving with 20 km/h. All configurations were carried out with and without a helmet and with and without the expandable B-Pillar.

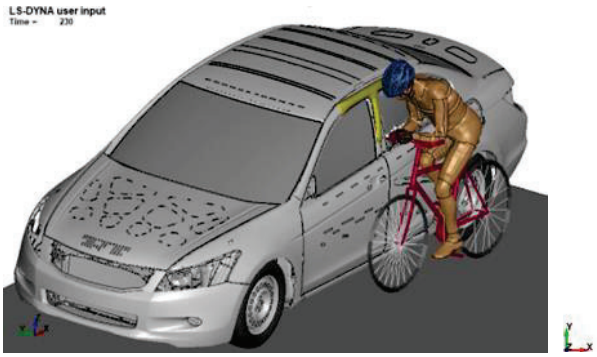

Figure 12a: Simulation of expandable B-pillar concept in LS-Dyna.

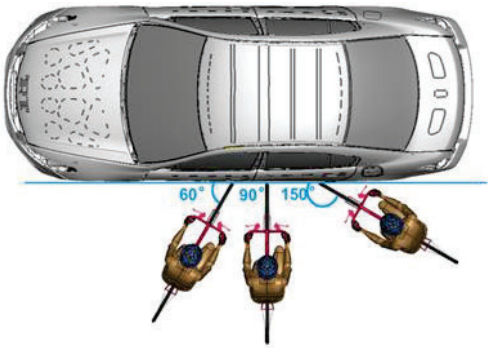

Figure 12b: Bicycle impact angle.

In Table 4, the head and neck results from the simulations where the vehicle is standing still are shown. In the configuration where the bicyclist had a 90° impact point to the vehicle the HIC15 (Head Injury Criterion, measured over 15 milliseconds) values were highest, followed by the impact angle of 60°. The expandable B-pillar reduces the AIS2+ head injury risk from 69% to 9% with 90° impact point and 28% to 2% in 60° (Table 4). In Table 5, the results from the simulation where the vehicle is moving with 20 km/h is shown. For more information see Carroll et al. (2022).

Table 4: Head and neck results from simulation where the vehicle stands still, with and without expandable b-pillar and with and without helmet

Position	**90˚**			**60˚**				**150˚**				
Vehicle Velocity (km/h)	0.0	0.0	0.0	0.0	0.0	0.0	0.0	0.0	0.0	0.0	0.0	0.0
Bicycle Velocity (km/h)	20.0	20.0	20.0	20.0	20.0	20.0	20.0	20.0	20.0	20.0	20.0	20.0
Helmet	No	Yes	No	Yes	No	Yes	No	Yes	No	Yes	No	Yes
Active Structure	No	No	Yes	Yes	No	No	Yes	Yes	No	No	Yes	Yes
Hic15	736	644	217	187	417	365	101	97	253	122	107	77
*Hic15 (AIS2+) %	68.9	57.7	8.6	6.5	27.8	21.8	1.8	1.7	11.3	2.8	2.1	0.9
BrIC	0.333	0.27	0.581	0.303	0.550	0.375	0.563	0.306	0.782	0.667	0.660	0.617
BrIC (AIS2+)	0	0	4.4	0	1.1	0	2.3	0	48.7	20.7	19.1	10.2
**MPS	0.146	0.207	0.212	0.228	0.197	0.178	0.254	0.119	0.538	0.553	0.357	0.297
MPS (AIS2) %	5.8	9.7	10.2	11.5	9.0	7.7	14.2	4.6	68.5	71.4	29.7	19.7
Nij (tf)	0.025	0.059	0.021	0.060	0.019	0.019	0.019	0.019	0.038	0.057	0.010	0.011
Nij (ce)	0.115	0.086	0.321	0.0	0.232	0.012	0.272	0.147	0.181	0.065	0.013	0.014
Nij (te)	1.160	0.969	0.918	0.834	1.065	0.869	1.106	0.885	0.689	0.513	0.919	0.718
Nij (cf)	0.148	0.136	0.136	0.138	0.125	0.131	0.124	0.127	0.064	0.123	0.022	0.021

**Injury risk calculated according to REF*
***MPS: Maximum Plastic Strain for gray material of brain*

Table 5: Head and neck results from simulation where the vehicle was moving 20 km/h, with and without expandable b-pillar and with and without helmet.

Position	**60°**		
Vehicle Velocity (km/h)	20.0	20.0	20.0
Bicycle Velocity (km/h)	20.0	20.0	20.0
Helmet	Yes	No	Yes
Active Structure	No	Yes	Yes
Hic15	513	190	168
*Hic15 (AIS2+) %	40.0	6.7	5.3
BrIC	0.913	0.828	0.854
BrIC (AIS2+)	75.2	59.2	64.6
**MPS	0.462	0.451	0.353
MPS (AIS2) %	52.2	49.6	28.9
Nij (tf)	0.053	0.070	0.090
Nij (ce)	0.052	0.282	0.196
Nij (te)	0.765	0.899	0.912
Nij (cf)	0.200	0.147	0.158

**Injury risk calculated according to REF*
***MPS: Maximum Plastic Strain for gray material of brain*

In D3.4 "Recommended design of the external protection system mounted on a vehicle will be reported together with a test report from the crash testing as well as a prototype demonstrator of the protection system" a prototype of an external airbag was created. A car approaching the bicycle from the rear is a common scenario, and the proposed airbag will be mounted to the side of the car covering the B-pillar area and the roof edge protecting the head and thorax of the cyclist in case of a crash. Three different airbag designs were evaluated by inflating the airbags mounted on a Body in White (BIW) (Figure 13a). The selected design was tested first with a headform (Figure 13b) and at a later stage on a crash track using a Hybrid III 50th percentile dummy on a standard bicycle. The same impact angles as in D3.3 were tested.

Figure 13a: Image of the inflated external airbag on top of the B-pillar, covering the roof edge.

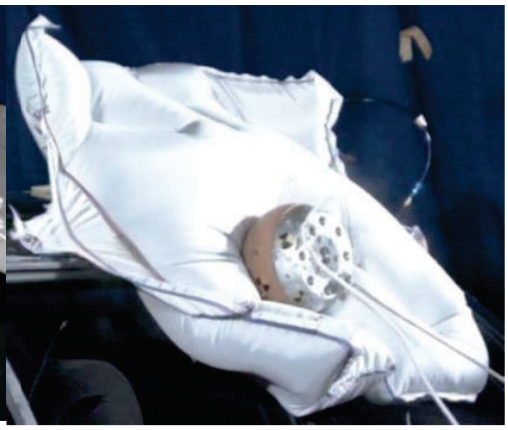

Figure 13b: Image of horizontal headform test with the inflated airbag.

The worst case for injury risk is where the bicyclist had a 90° impact point to the vehicle followed by the 60° impact point. In the 90° impact scenario, the airbag was reducing the HIC15 by 28%. More details about the tests and results can be found in Carroll et al. (2022).

In the deliverable 3.5, the possibility of combing Automated/Autonomous emergency braking (AEB) and Automated/Autonomous emergency steering (AES) system functionality was investigated for the overtaking scenario (Fig. 14). However, to reduce the complexity of carrying out simulation using simple vehicle dynamics models, the design of the collision avoidance system included AEB or AES implementation as a combined functionality (brake first and then steer). The decision making to activate AEB or AES system was based the presence or absence of an oncoming vehicle and the lateral overlap with the cyclist when the vehicle and the cyclist were on collision course. The selection of factors for decision making was based on the parameter analysis carried out and the review of steering functions. The emergency steering system designed in D3.5 delivers a lateral offset of 0.75 m (complying with UN ECE R79 regulation). However, to minimize the head-on collision with the oncoming vehicle, the assumption is made that AES is only activated when there is no oncoming vehicle, or if it is very far away and does not influence the overtaking process. In situations where AES is not possible to activate and avoid collision, AEB is proposed.

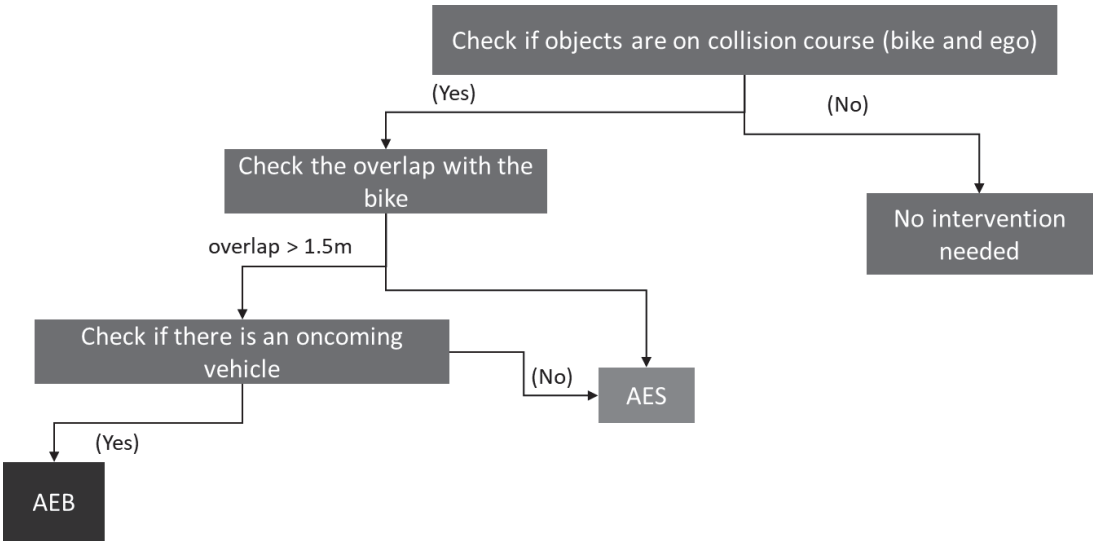

Figure 14 Decision tree used to active either AEB or AES when the threat is detected.

In conclusion, WP3 leveraged the models from WP2 and the crash scenarios from WP1 to create prototypical safety systems. The safety systems included active safety (e.g., warning and steering/braking intervention) and passive safety (external airbag and expandable pillars). The benefit of these safety systems was evaluated in WP4. In other words, the main contribution of this WP to the project and to the FFI program goals was prototyping new active and passive safety systems. The active safety systems used the models from WP2 to improve their acceptability.

6.4 WP4 – Results and deliverables

As part of M4.2, a simulation frame was defined to guide the safety benefit estimation of system developed in WP3. Figure 15, details the connection between the data used and the connection between the different components of the simulation.

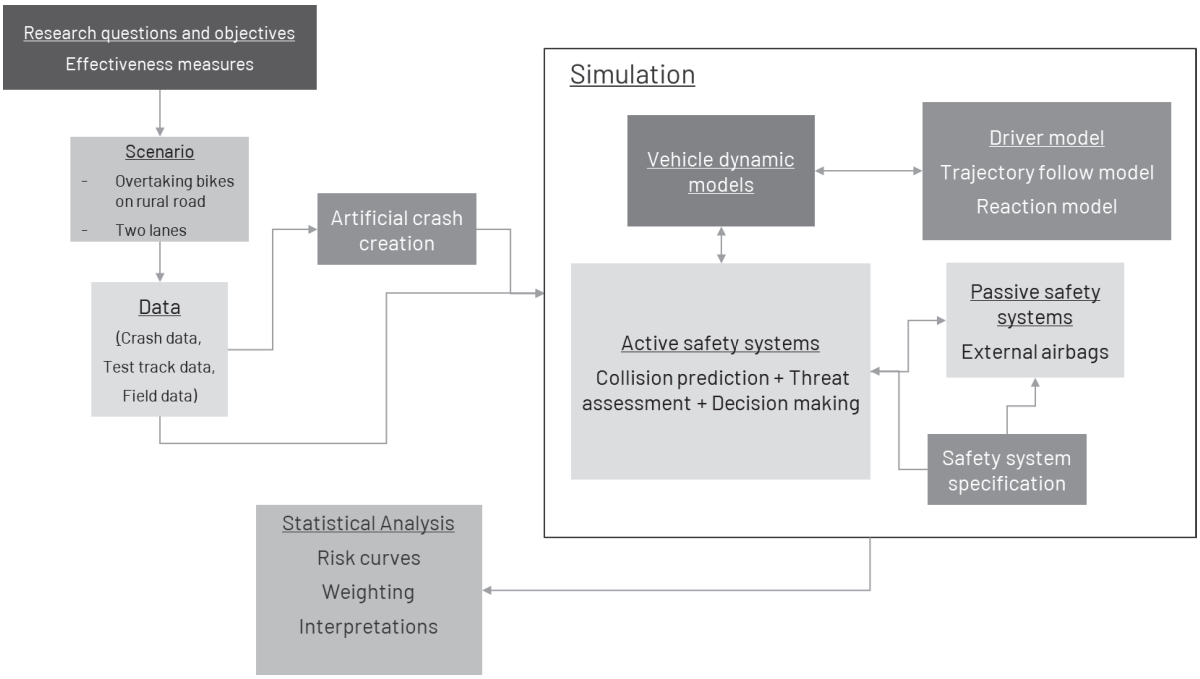

Figure 15 Framework defined during the WP4 to evaluate different safety systems.

The updated injury risk curves "D4.1, I Injury risk curves for lateral car to cyclist impacts" are based on the same filtering, weighting steps and method for creating injury risk curves that were used in D1.2 "Injury risk curves for lateral car to cyclist impacts" but were updated using the latest GIDAS release, August 2021.

6.4.1 Passive safety systems

Looking at the results from the simulation with the expandable B-pillar (as reported in D3.3) we can see that there is a substantial decrease in HIC15 and the risk of an AIS2+ head injury from injury risk curves created by NHTSA (NHTSA, 1995), Table 6. In the same table the HIC values from tests with the external airbag (as reported in D3.4) are shown and a clear difference without and with the airbag can be seen.

Table 6: HIC values from simulating expandable B-pillar and head impact test without and with external airbag.

		HIC_{15}	**AIS2+ head injury risk%**
Expandable B-pillar	**No active structure**	736	69
	Active structure	217	9
External airbag	**No airbag**	1614	99
	Airbag	228	9

To be able to estimate the effectiveness of an airbag or expandable B-pillar the data had to be re-calculated, and the injury risk curves re-drawn using a shift method similar to Liers and Hannawald (2011). In this way, the new number of injuries will tell us what the effect could be if the cars were equipped with the new passive safety system. The expandable B-pillar is mainly protecting the head impacting the side of the car and the "imaginary" protection system is assumed to reduce the AIS head level on the AIS scale by 2 if no helmet was worn. If a helmet was used or helmet use was unknown in the original sample, the AIS level is decreased by 1 (no effect any other body regions). Similarly, the external protection system is designed in such a way that it is protecting both the head and the thorax. The imaginary airbag will decrease both head and thorax injury by two levels on the AIS scale if no helmet or other protective clothing was worn. If a helmet or other protective clothing was worn, the AIS level was reduced by 1. The external protection system is assumed to absorb a lot of energy from the impact and is assumed also to reduce the injury sustained by ground impact. This is an assumption, and more research is needed in this question.

The results from the logistic regression are shown in Table 7. The baseline model is the same as the MAIS2+ injury risk curve in section 2. In Figure 16, the risk curves for the baseline, imaginary expandable B-pillar and imaginary airbag are shown.

Table 7: Result from logistic regression, std. Error and p-value, for MAIS2+ for the different models in same direction car-to-bicycle crashes.

Model		Best estimate	Std. Error	p-value
Baseline	b_0	-1.922	0.258	<0.001
	b_1	0.040	0.010	
Imaginary expandable B-pillar	b_0	-2.29	0.291	<0.001
	b_1	0.030	0.011	
Imaginary airbag	b_0	-2.496	0.311	<0.001
	b_1	0.030	0.011	

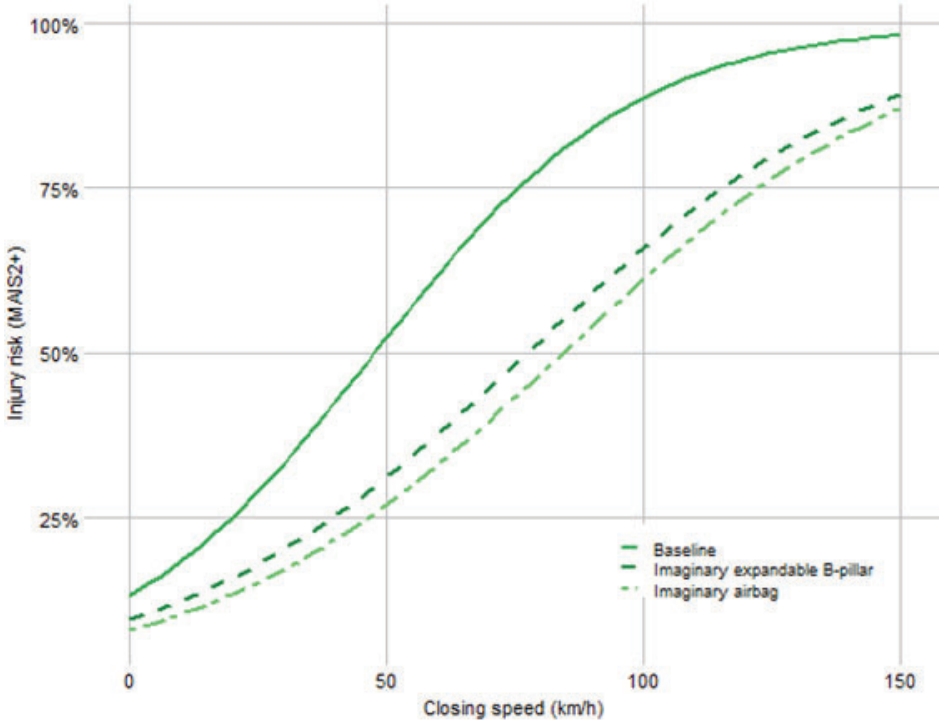

Figure 16. Injury risk curves for MAIS2+ with cars equipped with the different safety systems in same direction car-to-bicycle crashes.

6.4.2 Active safety systems

The safety benefit of a state-of-the-art AEB alone and in combination with in-crash protection (developed in WP3) to address these crash scenarios was predicted. To do so, the injury risk curves created in D4.1 – Injury risk curves for car-bicycle side impacts with in-crash protection devices – were used. The overtaking crashes extracted in WP1 that were available in the GIDAS Pre-Crash Matrix data (PCM) were simulated in Autoliv's in-house simulation tool KIIAS (Kinematic Investigation of Injury Avoidance by Simulation) (Jeppsson & Lubbe, 2020) based on Matlab scripts. Crash avoidance and speed reduction were translated into injury and fatality reduction via the injury risk curves.

GIDAS data released in August 2021 was used for this study from which a sample was selected as in D1.1. Crashes with unknown closing speed, which is defined as the vector difference between impact velocity of one vehicle and the velocity at the centre of gravity of the other vehicle just prior to an impact, were removed as well as unknown Maximum Abbreviated Injury Scale (MAIS) level, 2015 version. This resulted in a final sample of 295 crashes. (Twelve more than in D1.2.)

The German In-Depth Accident Study Pre-Crash Matrix (GIDAS-PCM) contains a selection of two participant crashes from the GIDAS database. The crashes contain details of the trajectories of both participants involved as well as reconstructed data. Data for the final seconds before the crash is reconstructed with a sample frequency of 100 Hz (Erbsmehl, 2009). In GIDAS-PCM, a diamond shape is used to represent a cyclist, where the widest part is the handlebar of the bicycle (VUFO, 2019).

Data from the GIDAS-PCM was extracted to match these crashes and resulted in a sample of 170 overtaking crashes for simulation.

The results from the simulations show that the Reference AEB was activated in one third (34%) of the crashes and that one fifth (20%) of the crashes were completely avoided with the AEB. Increasing the FoV to 179° there was only a slight increase by the numbers where the AEB activated to 36%, but no change regarding injury risk or speed reduction, which indicates that this parameter is not the most important one in scenarios where a bicycle is being overtaken by a passenger car.

With the Reference AEB, the risk of sustaining an MAIS2+ injury was reduced from 35% without AEB to 27%. Adding the imaginary expandable B-pillar reduce the risk from 22% to 16% with the AEB and adding the imaginary airbag reduce the injury by another 4% and 2% respectively (Table 8).

Table 8: Average risk of MAIS2+ injury depending on model and if AEB was present or not.

Model	No AEB	AEB
Baseline	35	27
Imaginary expandable B-pillar	22	16
Imaginary airbag	18	14

The original average collision speed was 31.1 km/h, by adding an AEB system, the average collision speed was reduced by 7.9 km/h to 23.2 km/h. Almost all crashes with a collision speed above 50 km/h remains even with the AEB, which suggest that the system is most effective in lower speeds.

In the deliverable 4.3, simulations were carried to predict the safety benefit of AEB and AES models developed in D3.5 using artificial crash data and naturalistic data collected as part of WP5. Artificial crash data was created using, test track data collected during MICA1 project. Trials were converted into artificial crashes by taking away the brake onset point for accelerative overtaking and the steer onset point for flying overtaking. From those points onwards, the speed was assumed to be constant until the end of the trial; the heading angle of the car was set to 0, meaning that the ego car continued to go straight ahead until it collided with the bicycle. By taking away the driver's actions, we assumed that drivers are distracted, which leads to rear-end collision with the bike. For

both the bicycle and the oncoming vehicle, the positions and speeds were also kept as they were at the time the driver started to either brake or steer away. Naturalistic data was collected on the rural road Spårhagavägen, Mölndal, Sweden, from 2021-08-30 to 2021-09-05. The road is a two-lane rural road with speed limit 70 km/h. The road has a solid line stretch in western direction (dashed in eastern direction), prohibiting overtaking during that stretch (only in western direction) using four Viscando smart traffic sensors.

Data	TP	FP	TN	FN
Artificial crash data (Test track)(102)	100%	0%	0%	0%
NDS data (90) (Viscando)	0%	0%	100%	0%

Data	Nr. of AEB	Nr. Of AES
Artificial crash data (Test track)(102)	53%	47%

Data	TTC based				BTN based	
Nr. Of collision avoided	1.7s	1.2s	1s	0.7s	BTN > 1	
Artificial crash data (Test track)(102)	100%	100%	94%	94%	0.95s	93%

In D4.4, the safety benefit estimation of combined Automated/Autonomous emergency braking (AEB) and Automated/Autonomous emergency steering (AES) alone and in combination with in-crash protection system based on GIDAS-PCM was carried out. The results simulation is also scaled and extrapolated. The simulation was carried out based on the evaluation framework proposed in M4.2. For two crashes the simulation did not work, so 168 out of 170 crashes were simulated. Hence these two trials were excluded from the simulation results. Tables below show the performance of the models used for calculating safety benefit.

Table 9: Classification of the type of activation from the simulation.

Data	TP	FP	TN	FN
GIDAS – PCM (168)	96%	0%	0%	4%

Table 10: Type of system activated based on the decision tree implemented.

DATA	NR. OF AEB	NR. OF AES
GIDAS – PCM	21%	79%

Table 11 shows the number of crashes avoided by either the AEB or AES system when activated. The effectiveness results show that earlier activation of the system (TTC = 1.7s) results in 80% of the crashes being completely avoided. As the activation time gets smaller (closer to the bike) the number of collisions avoided goes down to 77% (TTC-based activation). Similarly, BTN-based activation, where the mean activation time of 0.6s results in the lowest number of collisions avoided (40%).

Table 11: Number of collisions avoided for all the TP activation observed based on different methods used for activation of the system.

DATA NR. OF COLLISION AVOIDED	TTC BASED				BTN BASED	
	1.7s	1.2s	1s	0.7s	BTN > 1	
GIDAS – PCM	82%	83%	81%	76%	0.6s	44%

The weighted effectiveness of the different AEB/AES systems without and with the presence of an imaginary expandable B-pillar or imaginary airbag can also be found in Table 12. The effectiveness varies between 76% and 83% for the baseline system and between 87% and 91% with the imaginary airbag.

Table 12: The average weighted collision speed and MAIS2+ effectiveness depending on the AES/AEB model and the presence of a passive safety system.

	PROPORTION OF AVOIDED CRASHES	AVERAGE SPEED REMAINING CRASHES (KM/H)	EFFECTIVENESS AES/AEB (%)	EFFECTIVENESS AES/AEB + IMAGINARY EXPANDABLE B-PILLAR (%)	EFFECTIVENESS AES/AEB + IMAGINARY AIRBAG (%)
TTC 1.7S	82	31.2	82	89	90
TTC 1.2S	82	28.8	83	90	91
TTC 1S	80	29.8	81	89	90
TTC 0.7S	78	33.7	76	85	87

A comparison between Swedish *If* data and German GIDAS data on different injury levels was conducted – only minor differences could be found between the two databases, Table 13. This means that any conclusions that can be drawn for Germany also applies to Sweden.

Table 13: The share of injury levels comparison between If and GIDAS divided.

	GIDAS	*IF*
MAIS3+	8.232	10.66
MAIS2	21.037	16.39
MAIS0-1	70.732	72.95

In conclusion, WP4 estimated the safety benefits of active (AEB/AES) and passive (expandable pillar and external airbag) safety systems. In other words, the main contribution of this WP to the project and to the FFI program goals was showing the

potential benefit of prototypical safety systems developed in MICA2. While most of the safety benefit estimations were made with simulations, Autoliv also used experimental data from crash tests.

6.5 WP5 – Results and deliverables

6.5.1 Driver + Vehicle in-loop (DVIL)

The introduction of more and more complex advanced driver assistance and autonomous drive systems (ADAS/AD) requires the development of efficient test methods both to aid the function development process with fast feedback on function performance, and to ensure the safety of the deployed function. User interaction with the AD/ADAS system is of great importance, as it affects the function effectiveness, real and perceived safety, and comfort.

Driving simulators provide a faster, safer, and more repeatable method to test driver behavior and interaction when compared to test track experiments. However, in standard simulators, the driver is not experiencing the real vehicle dynamics and the AD/ADAS functions, when present, are not the actual production functions. Driving simulators also tend to induce motion sickness in some scenarios, which can limit their use especially for long user studies.

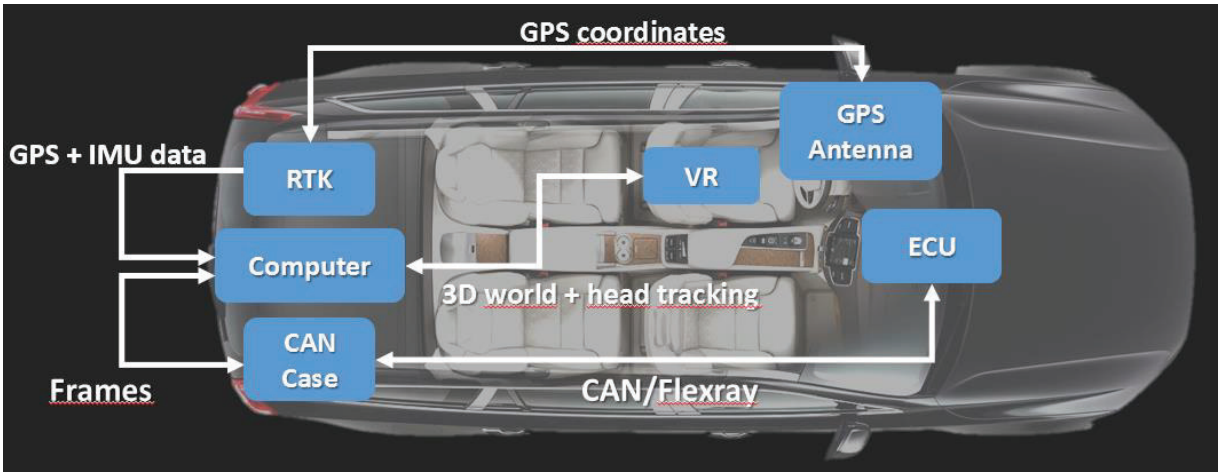

Figure 17: Implementation of DVIL architecture in Chronos 2 project

To overcome the limitations of driving simulators, Volvo Car Corporation (VCC) has developed a driver+vehicle in-loop (DVIL; Fig. 17) system aimed at testing assisted driving and active safety (ADAS) functions in dangerous scenarios. The system has been developed mainly during the Vinnova- funded FFI projects NGTest and Chronos 2.

In DVIL, the driver wears a virtual reality head-mounted display (HMD) while driving a real car on a test track. Both driver and vehicle are exposed and react to a simulated traffic scenario. The traffic scenario can either be generated by a traffic simulator software (VCC's own or other simulator), and then rendered with Unity in real time, or can be programmed directly in Unity. The simulation and rendering run on a PC installed in the vehicle. A real-time computer can also be added to run the traffic simulation if required.

The Chronos 2 implementation included two scenarios: 1) urban scenario with pedestrian detection and autonomous emergency braking; 2) highway scenario with collision warning and collision mitigation by braking. Other ADAS functions which are within the scope of DVIL include adaptive cruise control, pilot assist, and traffic jam assist.

A virtual reality headset (Oculus Rift in Chronos 2 implementation) is used to feed the virtual environment to the driver. The HMD position and orientation inside the vehicle are tracked by using only the inertial measurement units (IMU) of the headset. Drifts in the HMD orientation are corrected via a software, developed by VCC, which uses information of the car heading.

The vehicle's position is tracked via global positioning system (GPS) measurements with an accuracy of 1cm (with RTK3000 motion pack). IMUs in the vehicle are used to measure acceleration, pitch and roll. The position and orientation of vehicle and HMD are combined to obtain the pose of the headset in the rest frame. This pose is used by Unity to render the virtual world to the HMD.

Traffic objects, such as other vehicles and virtual road users (VRU; e.g., pedestrians), can be generated by the traffic simulator or directly included in Unity as game objects. A list of objects detected by the vehicle is compiled by a sensor model, which simulates the field of view and behavior of the on-board sensors (e.g., cameras, radars). This sensor model can be either a high-fidelity model in the traffic simulator, or an ideal model implemented directly in Unity 3D.

The list of detected objects includes object type, position, velocity, heading, and other information necessary to trigger the ADAS function under test. This information is sent to the vehicle's electronic control unit (ECU) via a controller area network (CAN) interface. The ECU reacts to the simulated objects by activating the appropriate ADAS function, as if the objects were real.

Signals from the internal car bus can be extracted via flexray interface and visualized in Unity in order to maximize the driver's immersion. In the current implementation, these include steering wheel angle, direction indicators, speed, revolutions per minute, and door state (open/closed). All signals on the car bus can in principle be accessed if needed.

The road infrastructure is represented in Unity 3D and georeferenced to the real test track that is used in the experiment, to facilitate the scenario design and to ensure safety of execution.

ARCar

The Open Innovation Arena at Volvo Cars has developed a platform to evaluate human – machine interaction (HMI) with augmented reality (Fig. 18). The concept of the system is similar to DVIL, but uses a video-see-trough headset to visualize a virtual interior of the car. The headset, developed by Varjo, has low latency and human-eye resolution, which makes it possible to drive the car with the headset on in normal traffic.

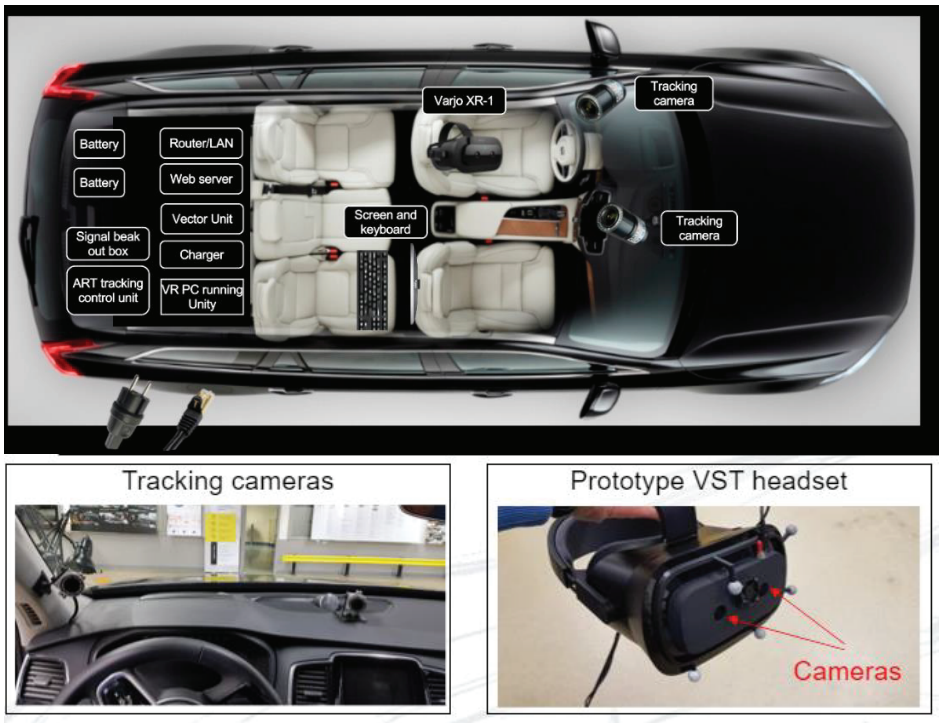

Figure 18: Implementation of ARCar at Volvo Cars Open Innovation Arena.

Compared to the DVIL setup, the system has better resolution and can provide both VR and AR experiences, but lacks the capability to inject virtual targets to the active safety ECU, or visualize a georeferenced road infrastructure.

A new simulator for MICA 2

For the MICA 2 project Volvo Cars developed a new simulation environment based on the capabilities of DVIL and ARCar. In the new setup, an updated ARCar was used as a base platform and a modified DVIL Unity 3D software was used to run and visualize the scenarios.

Updates of ARCar hardware platform

In order to increase the heading accuracy and minimize heading drift, the motion pack RT3003G was upgraded with a dual antenna configuration.

The AR/VR headset was upgraded to Varjo XR3 [https://varjo.com/products/xr-3/] which provides a nearly human eye resolution of 70 pixels per degree (ppd) and a wide field of view of 115 degrees. The new headset also has eye-tracking capabilities that allow for gaze studies.

DVIL Software platform updates

In the original DVIL setup signals from the car network were routed to the real time software platform via a CAN box + Canoe solution, while ARCar uses MQTT. In order to run the DVIL software on the new platform we implemented a Unity 3D data management plugin to read signals from the car network and modified the DVIL platform accrodingly. Signals of interest included: Acceleration pedal angle, Brake pedal angle, Speed, Vehicle indicator, Steering wheel angle, Gear selection.

To improve user immersion and provide realistic visual cues during data collection we implemented mirror reflections in rear and side mirrors (Fig. 19). Different solutions were investigated, including reflection probes and multiple cameras. The best and most computationally feasible solution was found to be to place different cameras at the mirror positions and use the render-textures function in Unity 3D.

Figure 19: Interior of MICA2 DVIL, with added reflections in rear and side mirrors.

The MICA2 cyclist overtaking scenario was developed as a Unity 3D project. The logics controlling the oncoming vehicle and cyclist, as well as the scenario configuration files, were implemented as C# scripts. An example of the scenario logics and configuration is

shown in Figure 20**.** Parameters for the scenario included lateral overlap ego vehicle to cyclist, time to collision between ego and cyclist, speed limit for ego.

```
/// <summary>
/// To set up the scenario
/// </summary>
/// <param name="overlap">latral overlap for the egocar and cyclist</param>
/// <param name="TTC">time to collision between egocar and cyclist</param>
/// <param name="SpeedLimitKMPH">the speed limit for the ego car</param>
 void ScenarioSetup(int overlap, int TTC, int SpeedLimitKMPH)
 {
     speedLimit = SpeedLimitKMPH;

     // Setting the cyclist lateral position according to the defined lateral overlap
     if (overlap == 0) cyclist.transform.position += new Vector3(egocarWidth / 2 + cyclistWidth / 2, 0, 0);
     if (overlap == 25) cyclist.transform.position += new Vector3(egocarWidth * 0.25f, 0, 0);
     if (overlap == 50) cyclist.transform.position += new Vector3(0, 0, 0);

     egoTargetCarTTC = TTC;
     TargetCarVR.Instance.MaxSpeed = SpeedLimitKMPH;

     // Select the speed limit sign to visualize
     if(SpeedLimitKMPH == 50)
         GameObject.Find("road_sign_speed_limit_70").SetActive(false);
     else
         GameObject.Find("road_sign_speed_limit_50").SetActive(false);

     // Calculate the initial position for the oncoming car
     float time_to_meet_egoCyclistTTC = (photocellToCyclistDis - CyclistVR.Instance.DisDiff - egoCyclistTTC * (SpeedLimitKMPH - 20) / 3.6f) / ((SpeedLimitKMPH - 20) / 3.6f);
     float iniDis = (egoTargetCarTTC + time_to_meet_egoCyclistTTC) * SpeedLimitKMPH / 3.6f * 2;

     // Set the initial position of the oncoming car
     targetCar.transform.position = new Vector3(targetCar.transform.position.x, targetCar.transform.position.y, iniDis + PhotocellToEgoDis);
 }
```

Figure 20: Configuration script for the MICA2 scenario in Unity 3D.

The 3D Environment in MICA2 DVIL was designed to look like the one in the VTI driving simulator to make it possible to compare user studies with the two systems. The 3D assets from VTI simulator were converted from .osgb to .fbx format and then imported into Unity 3D, see Figure 21.

Figure 21: MICA2 DVIL 3D scenario showing the cyclist and oncoming vehicle.

To be sure that the scenario would fit in the available driving surface, the 3D road was georeferenced to the Vårgårda airfield. In order to do that, we measured the GPS coordinates of the start and end positions on the airfield, as well as its orientation and we created a 3D replica in Unity 3D. The position of the ego car in the scenario was computed by the Unity 3D real time software by comparing the GPS coordinates from the RT3003G and the starting position coordinates of the airfield, see Figure 22.

Figure 22: Georeferencing of the road in Unity 3D to the driveable area at Vårgårda airfield.

In order to ensure safety, we introduced warning signals that are shown to the driver through the hadset. The conditions to show the warning signal are:

Condition	**Warning message**
Ego too close to end of road	Warning Stop !!!
Lost connection to motion pack	Warning Stop !
End of scenario	Slow down and Stop

In order to collect quantitative data for MICA2 user studies we implemented a logging application in Unity 3D. Relevant signals are logged every 20 milliseconds and include:

Signal	**Definition**
TimeStamps	System time in seconds
Ego Car Position X, Z	Position of center of ego car in meters
Ego Car Heading	North-East Ego heading relative to road direction in degrees

Acc Pedal Angle	Angle of accelerator pedal in degrees (0 = rest position)
BreakPedal	Boolean: is brake pedal pressed?
BreakPedalAngle	Angle of bralke pedal in degrees (0 = rest position)
Speed kmph	Speed in km/h from car network
Speed mps	Speed in m/s from Unity 3D
Speed GPS mpsN; Speed GPS mpsE	Speed along North and East in m/s from GPS
Vehicle Indicator	Turn indicator on/off from car network
Acceleration Y; Acceleration X	Longitudinal (Y) and lateral (X) accelleration in m/s^2 from car network
Steering Wheel Angle	Angle of steering wheel from center position in degrees, clockwise
Target Car Speed	Speed of oncoming vehicle in m/s
Target Car Max Speed	Max speed of oncoming vehicle in km/h
Target Car Position x; z	Position of oncoming vehicle in Unity 3D, meters
Target Car Heading	Heading of oncoming vehcle
Cyclist Speed	Speed of cyclist in m/s
Cyclist Position x; z	Position of cyclist in Unity 3D, meter
Cyclist Heading	Heading of cyclist

Testing augmented reality

The Varjo headset has augmented reality (AR) capabilities that allowed us to explore how AR may benefit DVIL. One obvious advantage of AR over VR is safety, as the driver is seeing the actual drivable surface and is aware of the surroundings, making him/her less dependent on the safety driver.

In order to enable AR in DVIL we created a separate Unity 3D project containing only the cyclist and oncoming vehicle and we added a mask to replicate occlusion from the interior of the vehicle See Figure 23.

The system was tested at Hällered test track in the Summer of 2021, for further details see Vivek Vivian's Master thesis [https://www.diva-portal.org/smash/record.jsf?pid=diva2%3A1612542&dswid=-2057].

Figure 23: The MICA2 scenario in AR as experienced by the driver

Because of some internal calibration happening in the Varjo headset the scaling of distant objects appears to be wrong, which also affects the perception of speed in the scenario, see Figure 24. This effect is present to a different extent in both VR and AR, but is much more noticeable in AR where there is a mismatch between the perception of distance of real infrastructure and virtual targets.
We investigated different solutions to remove the wrong calibration, including:

Manual tuning

Tuning the vertical position of the virtual objects has an effect on the scaling. We found a linear relationship between the distance to the headset and the vertical offset applied by the Varjo calibration. This could have allowed to solve the problem by rescaling the Unity 3D project. However, we found this tuning to be dependent on the user, probably because of different heights, which made this solution unpractical for large user studies.

Projection Matrix

We have tried to customize the projection matrix of the Unity 3D camera but we found it to be overwritten by Varjo's camera calibration.

Graphic Compositor

We tried to use two cameras, one to render only virtual objects, i.e. cyclist and oncoming car, and the other connected to the Varjo headset. We then rendered the two cameras together by using unity camera stacking[1]. However, we found that the augmented reality functionality is disabled when using the graphic compositor in Unity 3D.

[1] https://docs.unity3d.com/Packages/com.unity.render-pipelines.high-definition@10.0/manual/Compositor-User-Options.html

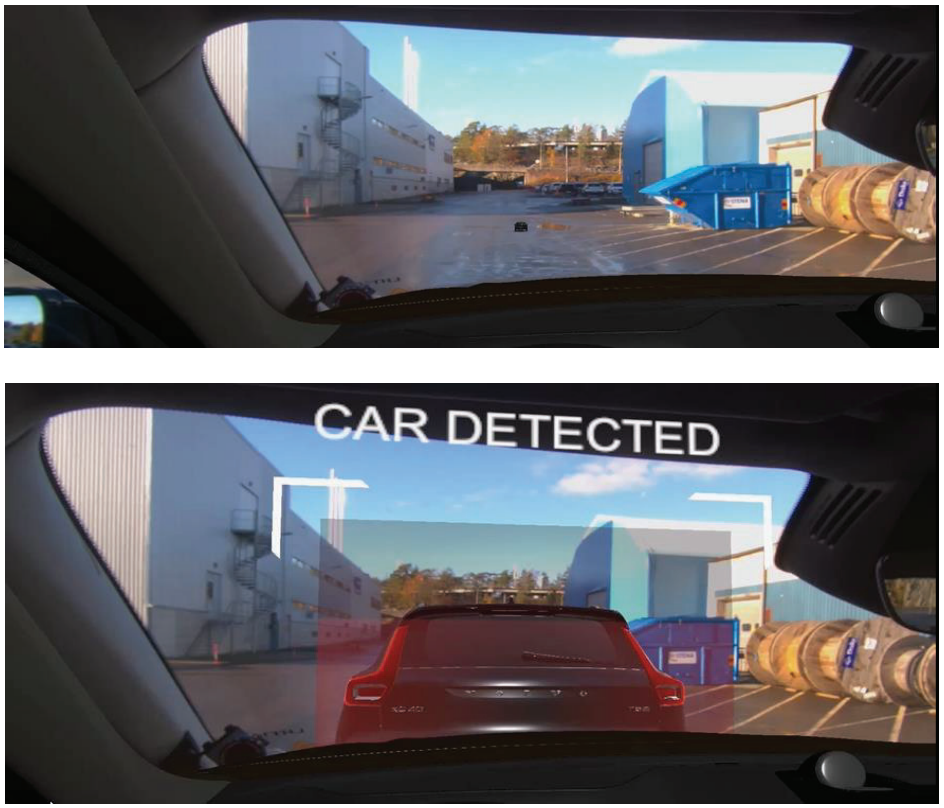

Figure 24: Experimenting with target scaling in AR.

We contacted Varjo but it was not possible to solve the AR scaling problem in the timeframe of the MICA2 project. For this reason we decided not to use AR for MICA2 user studies and to use the more stable VR solution instead.

User study and Demo

Between April 24 2022 and May 6 2022 we conducted a user study in order to collect data for the comparison of different simualtion environments and validation of the DVIL system. The study took place at Vårgårda airfield and included 37 participants, each of them experiencing 12 different MICA2 scenarios. The varying scenario paremetrs were: 1) time to collision (TTC) to oncoming car : no oncoming, 9 s, 6 s ; 2) Speed limit: 50 km/h, 70 km/h ; Cyclist overlap: 0%, 50%; Bike speed: 20 km/h. The speed of the oncoming car was adjusted in order to reach the desired TTC. The results fo the user study are discussed in D5.4 .

The MICA2 DVIL system was demonstrated to project members and advisory board during the final project demo on May 2 2023. During the demo, about 20 people could experience the DVIL system in 2 different MICA2 scenarios.

6.5.2 Visualization and quantification of cyclist behaviour (D5.3)

This chapter is partly based on the recent article by Rasch et al., produced within MICA2 project and recently accepted for publication in Journal of Safety Research (Rasch et al., in press). Certain parts of the text and certain images from the article have been adapted with minor changes, with permission from the article authors.

Naturalistic data from location-based measurements with infrastructure sensors
Naturalistic data on behaviours and interactions of road users in real traffic is paramount for identifying patterns and risks in traffic safety, visualizing and explaining behaviors of road users, and developing measures for increased safety, through better traffic infrastructure or advanced driver assistance systems (ADAS) in vehicles. Compared to both simulators and test track experiments, it has a superior ecological validity, that is, ability to capture the broad spectrum and statistical spread of real-life traffic scenarios and human behaviors. Moreover, simulators and test tracks can introduce various biases, stemming from a limited number of test persons, lack of realism, awareness of test persons about the test setup, to name a few. Naturalistic data can be free of these biases by design. For a detailed discussion of different types of data and comparison of naturalistic data to other sources, see Rasch (2023).

Test vehicles heavily equipped with sensors are commonly used for naturalistic data collection. During extended data collection campaigns, data on movements of host vehicle and surrounding road users detected by external sensors is collected in different road environments and weather conditions. The disadvantages of this method are: (i) high cost of equipment and data collection campaigns, (ii) driver bias, which means that the collected data reflects the driving behaviors of the particular vehicle drivers (who may not perfectly represent the spread of behaviours in the general population), and (iii) a large spread of road environments where the interactions of interest are observed, which makes it hard to separate the influence of human behavior-related factors from the ones stemming from the road infrastructure.

Location-based automated data collection using smart stationary sensors in the roadside infrastructure gives a number of advantages over in-vehicle data collection, such as:

- Lower cost and longer data collection time with minimum human effort
- Absence of driver bias, because interactions between large populations of road users over long time are collected

A shortcoming of the location-based data collection is small geographical coverage. Large road sections would require temporary installations of large sensor arrays, leading to high costs which are prohibitive for research community. However, increasing interest

from cities and road authorities to traffic measurement, monitoring and control using stationary GDPR-compliant smart sensors may soon result in more road sections, especially the ones critical for traffic safety, permanently equipped with such technology.

Because of limited area coverage, location-based data collection requires a careful choice of the location for data collection, in order to maximize the number of relevant events collected during the measurement period.

Viscando infrastructure sensor solution for naturalistic data collection

Viscando AB, a start-up from Gothenburg and a partner in MICA2 project, is specializing in collection of detailed traffic data and advanced traffic analysis – providing actionable insights on traffic flow and safety risks, real-time traffic control, as well as scenarios and reaction models for safer and more intelligent automated vehicles.

In MICA2 project, the naturalistic data collection was performed using 3D vision and AI-based infrastructure-based sensors OTUS3D developed by Viscando (see Figure 25). These sensors mounted on static roadside infrastructure like illumination poles or building walls, detect, classify and track all types of road users in their field of view, an example shown in Figure 25. For covering of extended road sections, a grid of multiple sensors can be used.

Figure 25: Left: a photo of Viscando OTUS3D sensor installed on a pole. Right: example of tracking of different road users in an urban environment.

A block diagram of the data processing in Viscando sensors is presented in Figure 26. Two embedded imagers take images 10-20 times per second. Then, proprietary 3D algorithms are used to calculate 3D position of each pixel. In the resulting dense point cloud, background and individual objects are separated in the segmentation step. A combination of statistical feature-based and appearance-based AI methods is used to classify each object. The available road user classes so far are the following: pedestrian, two-wheeler (including cycles, mopeds and e-scooters), light and heavy vehicles. Moreover, accurate size in all directions is calculated from the 3D point cloud for every

object. This gives rise to a 3D bounding box that tightly encloses the object and provides an accurate yet simple representation of the object extents.

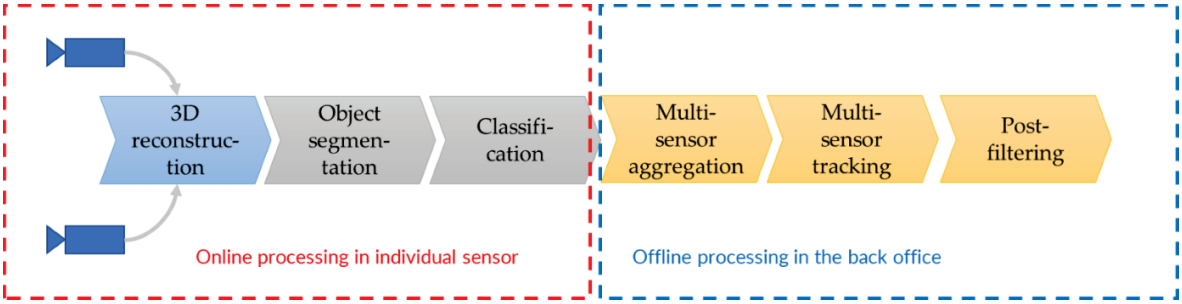

Figure 26: A schematic illustration of data processing steps in the Viscando 3D&AI based traffic sensing solution.

These steps are performed in real-time in the sensor's internal computational unit. At every measurement cycle, images are removed directly after 3D computation; thus, only object data that is stored and transmitted. As the object data only comprises position, size and type of the object, it is free from personal data – thus, no personal data is stored or transferred, ensuring compliance of Viscando measurement solution to General Data Protection Regulation (https://eur-lex.europa.eu/eli/reg/2016/679/oj , retrieved June 12, 2023).

Furthermore, in customized sensors used in research and development projects, there is also a possibility to store low-resolution and anonymized video. In such video, identification of persons and vehicles is impossible (hence GDPR compliance is preserved), while it is still possible to confirm the presence, type and the direction of motion. As it was important to both validate the data processing, and to avoid erroneous overtaking data in the analysis, such anonymized video was collected for manual annotation purposes in MICA2 project.

In the next step, object data from individual sensors are aggregated and combined, and tracking is performed on the aggregated data. A proprietary tracking method used by Viscando, called "offline tracker", utilizes the fact that data for the complete measurement period, rather than to a present time, is available; this enables tracker to better associate individual detections to object tracks, and to estimate the positions and speed more accurately – which, together with accurate 3D bounding box estimation, is a pre-requisite for reliable quantification of dynamic interactions between road users.

The object tracks are the final output of Viscando measurement system. The track data is stored in either hierarchical data format v5 (.h5, see https://en.wikipedia.org/wiki/Hierarchical_Data_Format) or in comma-separated (.csv) files, and contains the following information:

- Time stamp. The time is synchronized with NTP time server and is usually well aligned with GNSS time (this allows for a simple synchronization of Viscando data with other sources such as data from instrumented vehicles)
- Unique object ID
- Object class (pedestrian, two-wheeler, light or heavy vehicle)
- Position (x,y,z) in a ground-based coordinate system. In MICA2 project, a local coordinate system was defined; however it is possible to output positions in a GNSS-based coordinate system
- Velocity in x- and y-directions
- Heading angle
- 3D bounding box data, consisting of length, width and height of the bounding box enclosing the object.

Figure 27 shows snapshots for bounding boxes and anonymized video (panel a) as well as trajectories (panel b) as for a cyclist and a car in an overtaking event captured during the data collection. A video showing the dynamics of road users with detected positions, speeds and bounding boxes during the complete duration of overtaking event, is found here: https://www.youtube.com/watch?v=uLjw1yHNjwQ

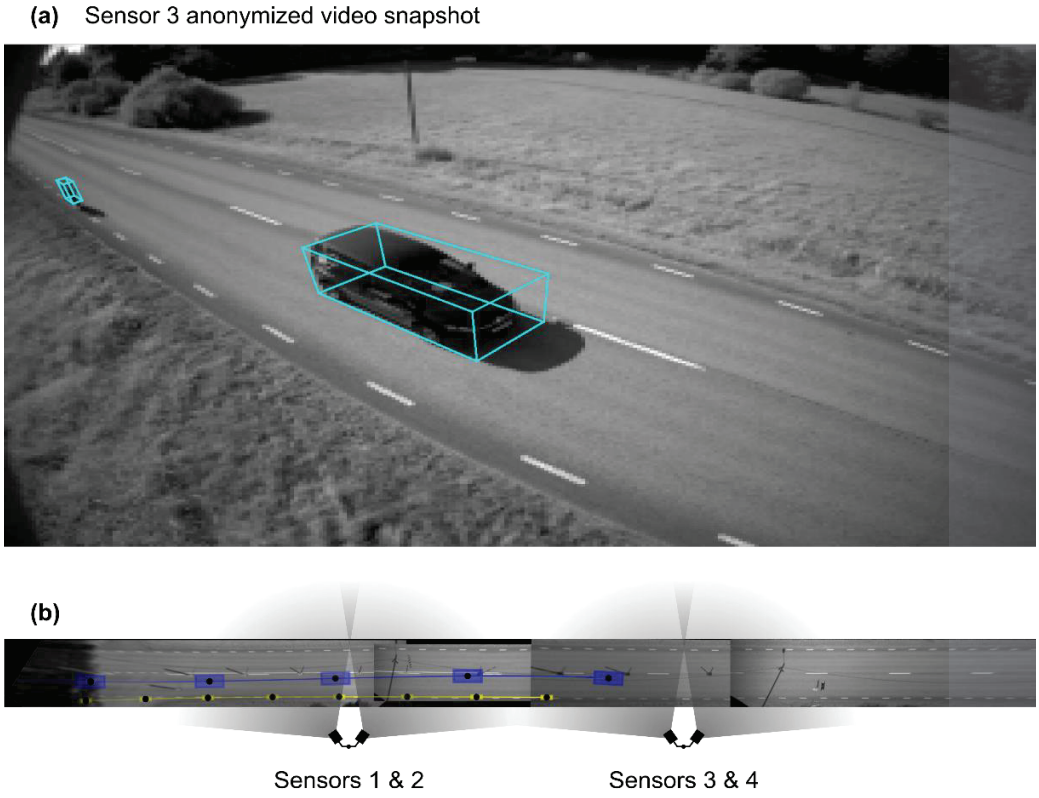

Figure 27: Data snapshot from an example overtaking maneuver. (a) Snapshot of anonymized video of the overtaking event, with 3D bounding boxes overlaid on the car and cyclist. (b) illustration of the sensor placement and trajectories of the car and cyclist involved in the interaction. Figure adapted from Rasch et al. (in press).

Improvements in Viscando measurement system within MICA2 project

Offline tracking and 3D bounding boxes. To ensure accurate and reliable data on interaction between cyclists and vehicles, Viscando put considerable effort into analyzing and improvement of the data quality. Specifically, the *offline tracking* and *3D bounding box calculation* algorithms, initially developed for the needs of automotive industry and optimized for vehicle interactions within the Vinnova financed projects Proof of Concept: Accelerated scenario data collection for AD verification (Diarienr. 2021-01135) and ASCETISM (Diarienr. 2020-05137) were tuned to better estimate positions, speeds and sizes of cyclists.

Viewer. Moreover, a viewer application was developed. The goal was to visualize and animate both trajectories and bounding boxes of the objects in 2D bird's-eye view and 3D camera-view, the latter combined with the anonymized video. Panel a in Figure 27 and the camera view in the corresponding video, present an example of visualizations provided by the viewer.

The viewer was successfully deployed and used for 2 main purposes:

- Analysis and tuning of the detection and tracking performance in Viscando measurement system
- Efficient manual validation of the automatically detected overtaking events, confirming presence, type, motion pattern of the object and assessing the accuracy of position and size estimates

Location choice

As the project scope allowed data collection only at a single location and for a limited period, an effort was put into identifying a suitable location, where sufficient amount of bicycle overtaking events could be captured. Such location should ideally have large flows of both bicycles and cars, and a suitable road layout without dedicated bicycle roads and with narrow shoulders. To reduce lead time and cost for installation and maintenance of the sensors, only locations in the vicinity of Gothenburg were considered.

To find candidate locations, interviews with project participants and cycling clubs were conducted, and information in media about cycling incidents have been examined. In the next steps, in-place observations during 2 hours at each of the 3 candidate locations were conducted to estimate the numbers of bicycles and vehicles.

Finally, a road stretch of Spårhagavägen, on the border between Mölndal and Gothenburg municipalities, was chosen (Figure 28). The investigated road stretch was straight and had a speed limit of 70 km/h (GPS coordinates of the center of the road stretch: 57.559778° latitude, 12.013694° longitude). The road had a lane width of about 3.6 m and connected two curve elements.

The curve element at the Western end of the observed road stretch resulted in a decreased sight distance for drivers moving towards west, which later showed to be an important aspect explaining overtaking behaviors (Rasch et al, in press). Furthermore, a solid line prohibited crossing the center line towards the Western end of the road (see the red-shaded area in Figure 28, d). The dashed line marks the edge of the lane and simultaneously the beginning of the road shoulder (Figure 28, c).

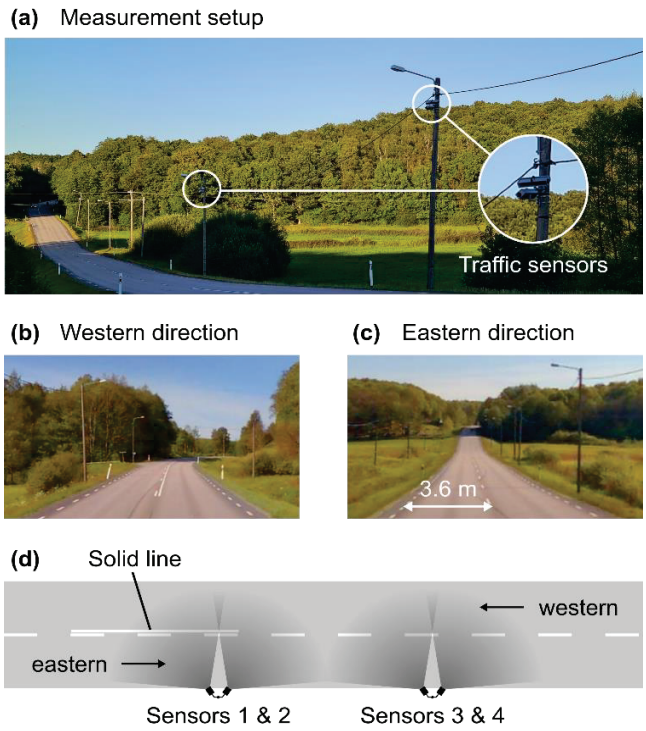

Figure 28. The segment of Spårhagavägen in Mölndal, chosen for the naturalistic data collection, and the setup of the sensor system. Panel a shows the road segment and how the four sensors were installed on two light poles. Panel b and c show the view from the center of the observed road stretch towards the Western and Eastern directions, respectively. Panel d shows the road layout and how the four sensors were oriented to cover the desired road stretch. The street images in panel b and c were obtained from Eniro[1]. Figure adapted from Rasch et al. (in press).

Installation of sensors and data collection

Viscando measurement system deployed at the chosen location consisted of four sensors mounted on two poles as seen from Figure 28 (a) and Figure 27 (b). The total length of the road stretch covered by the system was approximately 150 meters.

Viscando is grateful to Swedish Transport Administration (Trafikverket) for approval of the installation and data collection.

The data was collected during seven consecutive days, August 30th to September 5th, 2021. The collected data consisted of tracks of vehicles and cyclists, including their 3D bounding boxes, and anonymized video.

Visualization of bicycle behaviour

By plotting the trajectories and speed profiles of the cyclists involved in overtaking interactions (Figure 29), some aspects of the cyclist behaviours at the actual road stretch can be revealed.

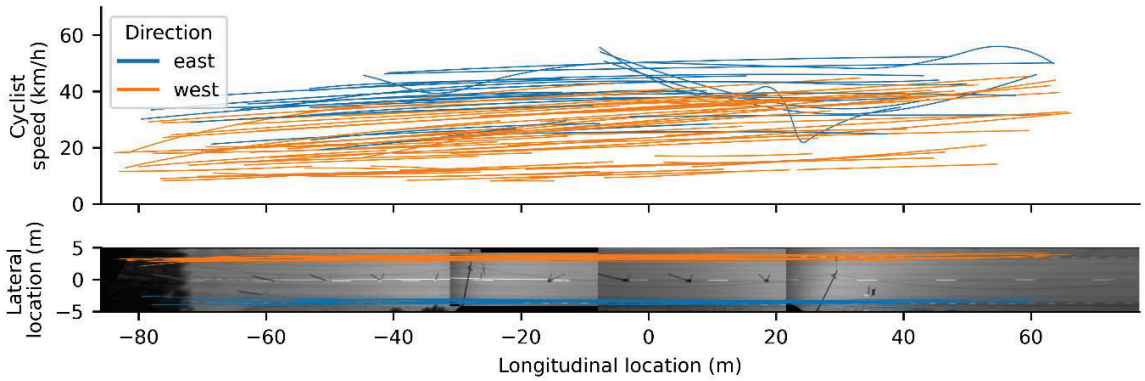

Figure 29. Visualization of trajectories (bottom) and speed profiles (top) of cyclists passing through the measurement stretch. Left corresponds to western direction.

First, the cyclists tend to cycle close to the vehicle lane edge – and often are moving in the vehicle lane, because of narrow shoulder. Because of this, vehicles during overtaking must move towards the opposite lane in order pass them with a sufficient lateral clearance. This increases risks for collision, either with the cyclist because of inadequate clearance, or with oncoming vehicles.

Second, the velocities are much higher for cyclists moving in the eastern direction, because of the slope in the same direction. A large variation of the bicycle velocities allowed to study the cyclist speed as a parameter for the overtaking model.

Extraction of overtaking events

Overtaking manoeuvres were identified by the following criteria: 1) a car and a bicycle traveled in the same direction, and 2) there was a passing moment when the car and bicycle were exactly next to each other. Most events represented overtaking of a single cyclist by a single car, but minor amounts of other types of events were identified:

- Overtaking of a cyclist by a heavy vehicle
- Overtaking of two or more cyclists moving in a group
- So-called piggybacking manoeuvres where a vehicle closely followed the one in front of it during the overtaking

These events were excluded from the further analyses to narrow the scope and to reduce the complexity of the modelling. However, these can be relevant for further studies focusing on more complex and infrequent interactions.

Validation of the overtaking events

Visual validation. We manually reviewed the recorded anonymized videos from the sensors for all overtaking events automatically identified using the algorithm presented above. This was done to verify that the cyclist was correctly classified and was not, for instance, a motorized scooter. Furthermore, using the viewer application described above, we confirmed that the bounding boxes qualitatively matched the actual road-user dimensions by visually verifying that the road user was well enclosed within the cuboidal box, without clear gaps or excesses.

Position and size accuracy. Position and size errors for light vehicles have been earlier assessed in similar environment (a straight section of an urban motorway with a similar speed limit 70 km/h) within the Vinnova financed projects Proof of Concept: Accelerated scenario data collection for AD verification (Diarienr. 2021-01135) and ASCETISM (Diarienr. 2020-05137), by comparing the measurement results with ground truth position data from test vehicles of known dimensions, equipped with high accuracy differential GNSS units (Oxford Technical Solutions RT3003, https://www.oxts.com/products/rt3000-v3/).

The lateral position and width errors are provided in Table 14 below. The reason for considering only lateral measures is that the accuracy of passing distance (lateral gap between car and bicycle) was in focus in the MICA2 project.

As it can be seen from the Table 14, the errors for cars are small and are not expected to have any influence on the results. Bicycle widths, on the other hand, are slightly overestimated, which may have resulted, on average, in shorter lateral clearances; however, it has been assessed that this systematic bias would not affect the general trends of driver behavior.

Table 14: Lateral position and width errors for cars and bicycles in Viscando measurements.

Value	Average error (m)	Standard deviation of error (m)
Car, lateral position	0,00	0,39
Car, width	0,05	0,09
Bicycle, lateral position	0,00	0,11
Bicycle, width	0,27	0,07

Summary of overtaking events

In total, automatic extraction of overtaking situations yielded 156 events. Manual validation removed a number of events with misclassified cyclists (typically mopeds or motorcycles detected as cyclists), unreasonable sizes of bounding boxes and faulty trajectories, which resulted in 127 confirmed events. After removing "special" event types mentioned above (heavy vehicles, piggybacking and groups of cyclists), 81 events with single bicycle being overtaken by single car, were available for behavior model development.

Table 15 summarizes these 81 overtaking maneuvers used for statistical analyses. Most of the overtaking maneuvers happened in the Western direction (Table 15, Figure 30). Cyclist and ego-vehicle speed were lower in the Western direction of the road, possibly due to the inclination of the road towards that direction. Figure 30 shows the locations of the overtaking maneuvers on the road stretch. Nineteen maneuvers were carried out in western direction during the solid-line segment, and in 14 of these maneuvers, the ego vehicle exceeded the solid line during the overtaking.

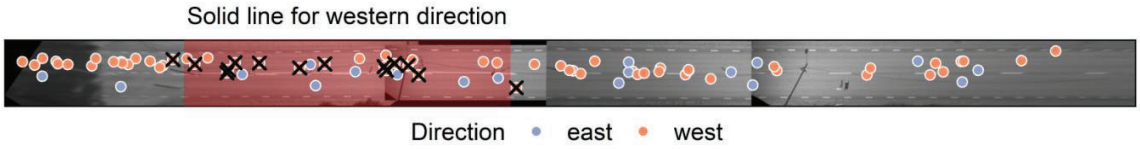

Figure 30. Overview of the ego-vehicle positions at the moment of passing the cyclist, plotted over the stitched camera images obtained from the traffic sensors. The red shaded area marks where vehicles may not cross the (solid) center line for the western direction. Black cross symbols mark where the ego vehicle exceeded the solid line during the overtake. Figure adapted from Rasch et al. (in press).

Table 15. Summary of the data used for statistical analyses, including the dependent and independent variables used for modeling. All data are measured at the return onset. All continuous variables are summarized as mean (standard deviation); all categorical variables as the number of samples per level (percentage). Square brackets indicate the range of values ([min, max]). Table adapted from Rasch et al. (in press).

	Direction of travel	
Characteristic	**east, N = 18**	**west, N = 63**
Presence of oncoming vehicle (-)		
Absent	9 (50%)	42 (67%)
Present	9 (50%)	21 (33%)

Lateral clearance (m)	2.26 [1.04, 3.34]	(0.68)	1.70 [0.49, 3.35]	(0.62)
Ego-vehicle speed (km/h)	75.5 [60.7, 98.2]	(9.9)	65.1 [37.2, 102.9]	(11.4)
Sight distance (m)	446.7 [382.1, 520.1]	(41.4)	197.9 [180.9, 255.0]	(20.4)
Distance to oncoming vehicle (m)	247.4 [28.7, 405.1]	(115.0)	118.4 [17.5, 209.5]	(60.4)
Not applicable	9		42	
Speed of cyclist (km/h)	10.5 [6.0, 14.3]	(2.3)	5.9 [2.3, 12.1]	(2.5)
Width of ego vehicle (m)	1.8 [1.6, 2.2]	(0.1)	1.8 [1.5, 2.2]	(0.1)

Qualitatively, drivers overtook with larger clearances when traveling at higher speeds (Figure 31). However, particularly in maneuvers performed at low clearance, cyclists were predicted to have perceived high risk during the passing (Figure 31).

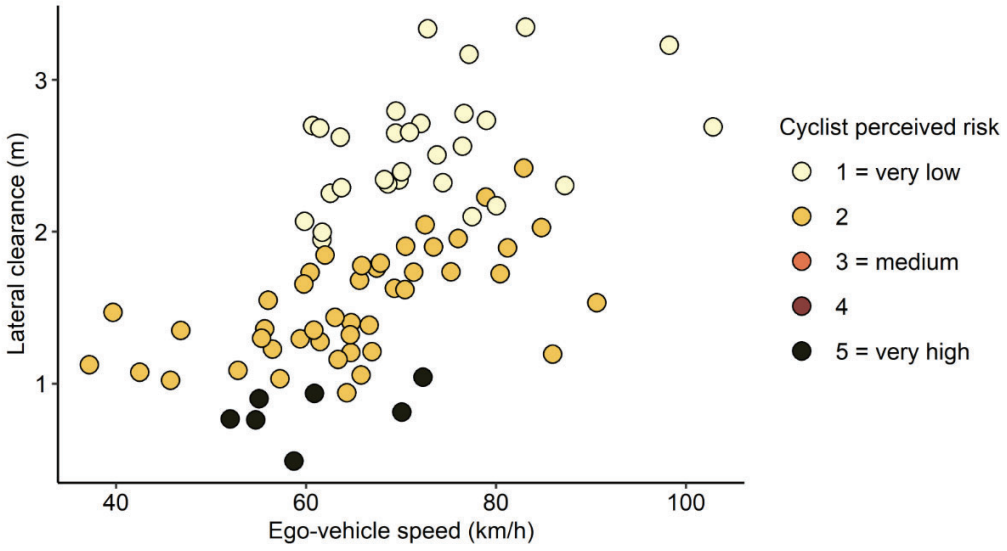

Figure 31. Lateral clearance and overtaking speed by drivers. The color indicates the perceived safety of the cyclist, predicted by the model developed by Rasch et al. (2022). Figure adapted from Rasch et al. (in press).

Use of extracted overtaking events for modelling and simulations.
The overtaking events proved useful for both driver modelling and benefit simulations, and were utilized for several of the project deliverables, as described in this report in the following sections:

- WP2, D2.3: Validation of the driver models built on test track data, on overtaking events from naturalistic data. Publication [Rasch, Flannagan, Dozza, 2022] is under review
- WP2. Model of the overtaking that is capable of prediction of passing distance and speed during overtaking in presence of oncoming vehicle and effect of the sight distance, described in detail in a recently published work by Rasch et al. (in press).
- WP4, D4.3. Simulations to predict benefit of safety systems performed on the overtaking events.

Conclusion: usefulness of location-based cyclist overtaking data
The traffic sensors used for naturalistic data collection in MICA2 project were roadside-based and, therefore, able to capture traffic continuously, in contrast to, for instance, airborne instrumentation like drones. This allowed the capture of a notable amount of overtaking maneuvers in shorter time (seven days) than other data-collection methods, such as naturalistic-driving studies that typically run over much longer durations and may be more costly (Kovaceva et al., 2019).

Furthermore, in naturalistic driving studies, drivers may be aware that they are driving an instrumented vehicle, which is a possible confounder that does not exist for roadside-based data collection. While not being able to capture driver-input signals such as steering-wheel angle or pedal controls, which naturalistic-driving studies usually do, roadside-based data collection allows for capturing the kinematics of all road users involved in the interaction and enable constraining specific infrastructure, which may favor analyses. This is particularly advantageous for overtaking interactions that are strongly influenced by the oncoming vehicle, whose position may be hard to estimate by on-vehicle sensors.

Roadside-based sensors are limited to their specific location and field of view. Even though our setup covered a stretch of about 150 m, we rarely captured all phases of an overtaking maneuver. While capturing the passing moment was central to studies that utilized naturalistic data in MICA2 project, future studies may need larger infrastructure sensor arrays. In addition, longer-term data collection should be performed in multiple locations in future studies, in order to obtain both more interactions and a better understanding of the role of different road designs. This puts the direction of the future work by Viscando – decreasing complexity and cost of data collection campaigns by

enabling easier installation, larger detection range (hence fewer sensors per location) and increased accuracy in data processing (to eliminate the need for manual validation).

Data dissemination
To enable further research on bicycle overtaking, Viscando is planning to provide access to both overtaking events and complete trajectory data to research community. As such, Viscando data including the dataset from Spårhagavägen, is a part of SAFER data catalogue, which can be accessed by all SAFER connected researchers[2].

6.5.3 Demonstration of cyclist overtake with virtual target injection (D5.4)

The main aim of the D5.5 was reconfigured to demonstrate the potential of an information/warning system to improve the lateral clearance (LC) (or passing distance) when overtaking a cyclist. The function was developed as part of D3.6 in WP3 (Development of active and passive safety systems). The aim of the information/warning system is to visually indicate the current LC to the cyclist during the approaching and passing phase of the overtaking.
From previous studies when cars are overtaking cyclist, due to large difference in the speed, the discomfort felt by the cyclist increases when the LC is low. The LC is defined as the distance between left extremity of the cyclist to the right extremities of the car. To minimize the risk and discomfort felt by the cyclist, several countries have implemented minimum passing distances. The minimum passing distances vary between 2 m to 1 m depending on the countries. As part of WP3, information/warning system concept was developed to help drivers to improve their minimum passing distance.

The system concept is based on different lateral clearance thresholds. The LC is obtained from the onboard sensors as part of object classification list. The information is presented to the drivers using the heads-up display. As the main is make sure greater than 1.5m LC is maintained, this value was set as one of the thresholds. If the driver is passing the cyclist with more than 1.5 m LC, it is indicated by showing a green bar on the heads-up display (see Figure 32). Similarly, two more thresholds were also set; a) yellow bar between 1.5 m to 0.5 m (see Figure 33) and b) red bar LC less than 0.5 m (see Figure 34). The colours are displayed in the heads-up display dynamically, meaning the LC is continuously calculated during different phases of overtaking and when the thresholds are met corresponding colours are displayed. The information about the LC is only presented to the driver 3 s TTC (time to collision); measured from front of the car to the rear of the bike, before approaching the cyclist and it is continuously monitored till the car has successfully passes the cyclist and is 2 s TTC away from the cyclist. The concept is implemented in the DVIL setup together with VCC and it was demoed during the final event of MICA2 project.

[2] https://tinyurl.com/SAFERDataCatalogue

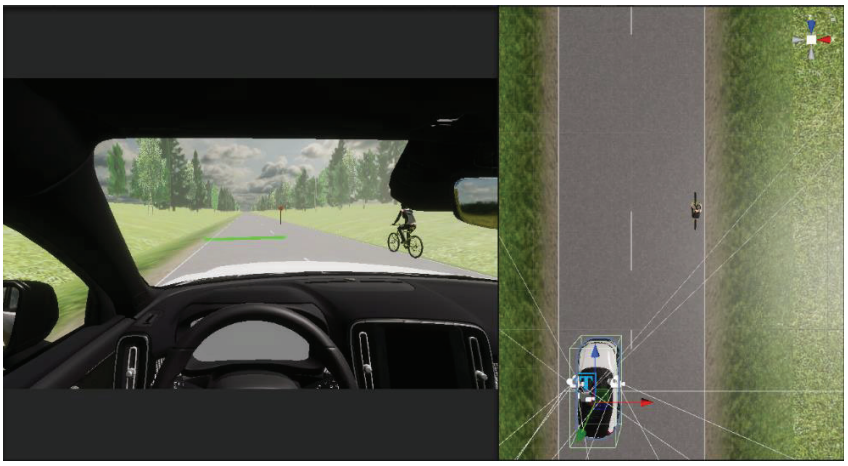

Figure 32: Green bar indicates - when lateral clearance is greater than 1.5m to the cyclist.

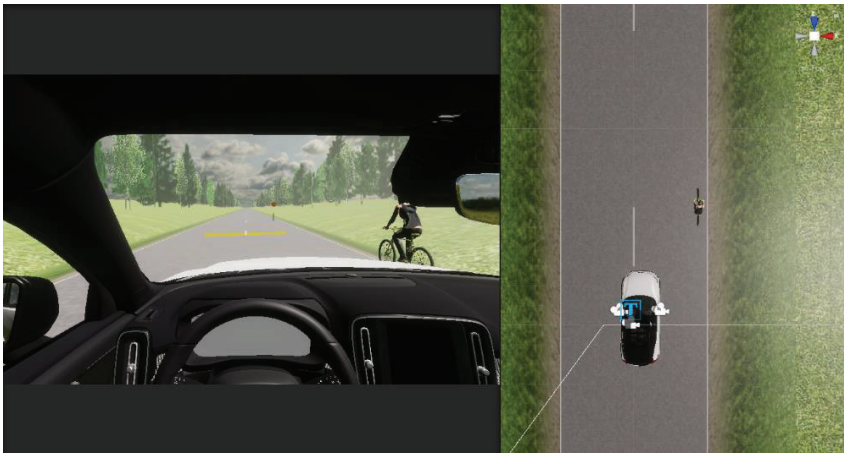

Figure 33: Yellow bar indicates - when lateral clearance is between 1.5 to 0.5m to the cyclist.

Figure 34: Red bar indicates - when lateral clearance is less than 0.5m to the cyclist.

The system concept that was developed and demoed during the project. During the demo the participants appreciated the concept and liked the idea being presented with

information that help promote safe overtaking of cyclist on a rural road. However, as this is an early concept, user studies have not been conducted as part of the development. Thus, the external validity of the concept is very limited. More research is needed to be carried out to understand the implementation and HMI related challenges.

In conclusion, WP5 performed several data collections while piloting and developing new test methodologies. WP5 also leveraged one of these new test methodologies (based on the use of virtual reality from a head-up-display on test-track) to demo some of the new active safety systems developed in WP3. Three main experiments provided data to WP2: 1) driving simulator experiment, 2) riding simulator experiment, and 3) test-track experiment. In addition, data from site-based naturalistic observation was also produced in WP5 and used in WP2 for model validation. It is worth mentioning that MICA2 collaborated with "Självkörande cyklar för mer realistisk utveckling och testning av system för cykelsäkerhet, diarienummer 2020-05133" where a robot bike was developed. The initial plan was for the robot bike to be used in experiments; however, because of technical problems, the experiments were not possible. Finally, while MICA2 planned to use both augmented and virtual reality on test-track, only the later solution (virtual reality) was viable. In fact, we had very hard time making the injected targets from augmented reality look realistic, possibly because the technology for augmented reality has yet to develop.

7. Dissemination and publications

7.1 Dissemination

How are the project results planned to be used and disseminated?	Mark with X	Comment
Increase knowledge in the field	x	2 PhD theses, 3 licentiate theses, and 15 more papers and conf. contrib. were published by MICA2.
Be passed on to other advanced technological development projects	x	Within Autoliv and Veoneer (now Magna) presentations have been held with leaders of advanced technological projects.
Be passed on to product development projects	x	Within Autoliv and Veoneer (now Magna) the project results were presented to the leaders of product development projects. Within Volvo Cars the results of the project will inform the choice of the best simulation techniques for product development at Volvo Cars. The aim is to enable early and safe testing of active safety and autonomous drive software in future cars.
Introduced on the market		
Used in investigations / regulatory / licensing / political decisions	x	The content of MICA2 was part of several presentations to regulatory and political decision-makers.

Through the advisory board links were established with Euro NCAP and UMTRI. The link with Euro NCAP may accelerate the introduction of MICA2 results in commercial products.

7.2 Publications

7.2.1 PhD Theses:

1. Kovaceva, J. “Methods and models for safety benefit assessment of advanced driver assistance systems in car-to-cyclist conflicts”, (2022), PhD Thesis, Chalmers University of Technology, Gothenburg, Sweden.
2. Rasch, A. (2023). Drivers overtaking cyclists and pedestrians: Modeling road-user behavior for traffic safety [Chalmers University of Technology]. https://research.chalmers.se/publication/534378/file/534378_Fulltext.pdf

7.2.2 Lic. Theses

1. J. Kovaceva, “Understanding and modelling car drivers overtaking cyclists: Toward the inclusion of driver models in virtual safety assessment of advanced driving assistance systems”, (2019), Licentiate thesis, Chalmers University of Technology, Gothenburg, Sweden.
2. Rasch, A. (2020). Towards computational models for road-user interaction: Drivers overtaking pedestrians and cyclists [Chalmers University of Technology]. https://research.chalmers.se/publication/518259/file/518259_Fulltext.pdf
3. P. Thalya - “Making overtaking cyclists safer - Driver intention models in threat assessment and decision-making of advanced driver assistance system” ,(2021) Licentiate thesis, Chalmers University of Technology, Gothenburg, Sweden.

7.2.3 Papers on International Scientific Journals:

1. Rasch A., Boda C.-N., Thalya P., Aderum T., Knauss, A. & Dozza, M. (2020) “How do oncoming traffic and cyclist lane position influence cyclist overtaking by drivers?”. Accident Analysis & Prevention, Vol. 142.
2. Kovaceva, J., Bärgman, J., Dozza, M. (2020). A comparison of computational driver models using naturalistic and test-track data from cyclist overtaking manoeuvres. Transportation Research Part F, 75, 87-105. doi: 10.1016/j.trf.2020.09.020.
3. Rasch, A., & Dozza, M. (2022). Modeling Drivers’ Strategy When Overtaking Cyclists in the Presence of Oncoming Traffic. IEEE Transactions on Intelligent Transportation Systems, 23(3), 2180–2189.
4. Kovaceva, J., Bärgman, J., Dozza, M. (2022). On the importance of driver models for the development and assessment of active safety: a new collision warning system to make overtaking cyclists safer. Accident Analysis and Prevention, 165, 106513. doi: 10.1016/j.aap.2021.106513.
5. PD. Fernández, M. Lindman, I. Isaksson-Hellman, H. Jeppsson, J Kovaceva. (2022). Description of same-direction car-to-bicycle crash scenarios using real-world data from Sweden, Germany, and a global crash database, Accident Analysis & Prevention 168, 106587

6.Moll, S., López, G., Rasch, A., Dozza, M., & García, A. (2021). Modelling duration of car-bicycles overtaking manoeuvres on two-lane rural roads using naturalistic data. Accident Analysis & Prevention, 160(July), 106317. https://doi.org/10.1016/j.aap.2021.106317
7. Rasch, A., Moll, S., López, G., García, A., & Dozza, M. (2022). Drivers' and cyclists' safety perceptions in overtaking maneuvers. Transportation Research Part F: Traffic Psychology and Behaviour, 84(July 2021), 165–176. https://doi.org/10.1016/j.trf.2021.11.014
8. Rasch, A., Flannagan, C., & Dozza, M. (2022). When is it Safe to Complete an Overtaking Maneuver? Modeling Drivers' Decision to Return After Passing a Cyclist. (submitted to IEEE Transactions on Intelligent Transportation Systems)
9. Rasch, A., Tarakanov, Y., Tellwe, G., & Dozza, M. (2023). Drivers passing cyclists: How does sight distance affect safety? Results from a naturalistic study. (Accepted for publication in Journal of Safety Research)

7.2.4 Conference contributions:

1. Thalya, P., Kovaceva, J., Knauss, A., Lubbe, N., & Dozza, M. "Modeling driver behavior in interactions with other road users", Transportation Research Arena, Helsinki, Finland 27-30 Apr 2020.
2. Kovaceva J., Thalya P., Lubbe N., Knauss A., Dozza M. "A new framework for modelling road-user interaction and evaluating active safety systems". 7th International Cycling Safety Conference, Barcelona, Spain, Oct. 10-11, 2018.
3. T. Aderum, S. Mastrandrea, J. Kovaceva, P. Thalya and M. Dozza. (2021). Driver response process when overtaking cyclists on European roads, 9th International Cycling Safety Conference, Lund, Sweden.
4. P. Diaz Fernandez, I. Isaksson-Hellman, H. Jeppsson, J. Kovaceva and M. Lindman. (2021). Description of same-direction car-to-cyclist crash scenarios using real-world data from Sweden, Germany, and a global crash database, 9th International Cycling Safety Conference, Lund, Sweden.
5. Rasch, A., Tarakanov, Y., Tellwe, G., & Dozza, M. (2022). Drivers overtaking cyclists on rural roads: How does visibility affect safety? Results from a naturalistic study. Contributions to the 10th International Cycling Safety Conference 2022 (ICSC2022), 66–68. https://doi.org/10.25368/2022.438
6. Mohammadi A., Piccinini G., Dozza M. (2022) " Understanding the interaction between cyclists and automated vehicles: Results from a cycling simulator study". 10th International Cycling Safety Conference, Dresden, Germany, Nov. 8-10 2022.
7. Rasch, A., Dozza, M. (2023). The effect of speed on driver behavior when overtaking cyclists: Results from driving-simulator and test-track data. ICTCT 2023 conference, Catania, Italy.
8. Mohammadi, A., Dozza, M. (2023). How do expert and non-expert drivers interact with cyclists at unsignalized intersections? Results from naturalistic data. 11th International Cycling Safety Conference, The Hague, the Netherlands.

7.3 Videos

The MICA2 **demo**: this video mainly describes the demo and was made mainly from footage collected at the final event:
https://www.youtube.com/watch?v=L7p0V9fvUPM

The MICA2 **project**: this video was created for the final event and describes the main results from the project:
https://www.youtube.com/watch?v=vmw2qZ3pIDo

The MICA2 work: in this play list some of the videos produced in MICA and MICA2 for dissemination purpose are presented.
https://www.youtube.com/playlist?list=PL4J_y4nKehcPSqrtaSYW2HDENCEMFwjT1

7.4 Presentations

Results from the MICA2 project were presented in several conferences, most notably at ICSC in 2019, 2020, 2022, and 2023 (panned).

MICA2 results were also presented within the SAFER network, providing periodic reports as a SAFER associated project and giving ad-hoc presentations, for instance on the SAFER day on March 10th 2023.

Finally, at the final event in Vårgårda on May 2nd 2023, the results from all WP were presented to several stakeholders.

8. Conclusions and future research

Leveraging multiple crash databases, MICA2 successfully developed and piloted prototype active and passive safety systems to make cyclist overtaking safer. Intelligent systems and automated driving functions may use the behavioural models from MICA2 to time interventions/warning and/or plan safe trajectories. The safety-benefit assessment from MICA2 clearly shows the potential of in-vehicle technologies to make cyclists safer. Within MICA2, several test environments have been developed and compared. Particularly interesting was the use of virtual reality on a test-track, which made it possible to test critical scenarios in a safe and repeatable way without compromising reality as much as in driving simulators. Naturalistic data were collected that revealed new insights in drivers' overtaking behaviour and enabled the validation of driver models fitted on ecologically less valid datasets.

Future studies should gather and combine larger data sets to further verify and validate the models and systems from MICA2. In addition, data from several countries may help appreciate the extent to which the models and systems from MICA2 may be tuned and adapted to different infrastructure and behaviours that may arise in different nations across Europe and the world.

The robot bike and cycling simulator that MICA2 experienced still need further development; however, their potential benefit for traffic safety research is undisputable. All project partners are pleased with the results and plan to continue the research activities performed in MICA2. Future studies may also expand the work from MICA2 by considering automated connected vehicles and addressing the cyclist point of view.

As long as overtaking maneuvers require for motorized vehicles to occupy the lane assigned to the oncoming traffic and/or to pass cyclists at close proximities, they will never be completely safe. Different compromises than the ones we have today for infrastructure design and its regulation—as well as for the kinematics adopted by the different road users involved in the overtaking—*can* make overtaking safer. In-vehicle technology may not change the infrastructure or its regulation, but it can favor safer kinematics. In particular, the results from MICA2 help explain 1) how machines can better estimate and promote trajectories that *maximize safety for all road users*, 2) when overtaking should simply *be avoided/postponed*, and 3) when *communication among road-users* (and with the oncoming vehicle in particular) may play an important role in making the maneuver viable and safer. More research and system development are needed to address these three critical issues and make overtaking safer. Euro NCAP may support the development of such research and systems by including scenarios where AES and AEB are challenged with multiple road users.

9. Participating parties and contact persons

9.1 Parties

9.2 Contact Persons:

Marco Dozza, Chalmers University of Technology, marco.dozza@chalmers.se, +46(0)317723621

Paloma Diaz Fernandez, Volvo Cars, paloma.diaz.fernandez@volvocars.com,

Alexander Rasch, Chalmers University of Technology, alexander.rasch@chalmers.se,

Prateek Thalya, Veoneer, prateek.thalya@veoneer.com,

Hanna Jeppsson, Autoliv, hanna.jeppsson@autoliv.com,

Yury Tarakanov, Viscando, yury@viscando.com,

Jesper Sandin, VTI, jesper.sandin@vti.se,

Magdalena Lindman, if, magdalena.lindman@if.se,

10. Acknowledgements

The MICA2 consortium is very grateful for the advice and support received from the advisory board. Thanks to Carol Flannagan for joining our meetings from the other side of the world, supporting our modelling efforts, and contributing to our papers. Rikard Fredriksson we appreciated your help connecting us with Euro NCAP and road designers at Trafikverket. These connections helped us understanding the role of infrastructure design on the naturalistic data we collected. The link with Euro NCAP helped our papers give sound suggestions for future protocols. Thanks, Natasha Merat, for participating to our meetings, supporting our work with positive feedback, and giving suggestions about the simulator experiments. Finally, Clay Gabler, unfortunately you were not able to participate to our meetings or to give us any advice because life decided so. MICA2 would have been a better project with your input, we definitely miss you.

Within MICA2, two PhD students graduated. We would like to thank the opponents Shan Bao from UMTRI and Chris Cherry from the University of Tennessee as well as all the members of the graduating committees: Tibor Petzoldt (Technical University of Dresden), Mette Möller (Technical University of Denmark), Aliaksei Laureshyn (Lunds Universitet), Mats Jonasson (Chalmers), Regine Gerike (Technical University of Dresden), Marco Pierini (University of Florence), Otto Anker Nielsen (Technical University of Denmark), and MariAnne Karlsson (Chalmers). Your feedback greatly improved our papers and our theses.

11. References

AbuAli, N., & Abou-zeid, H. (2016). Driver Behavior Modeling: Developments and Future Directions. *International Journal of Vehicular Technology*, *2016*, 1–12. https://doi.org/10.1155/2016/6952791

Adelberger, D., & Re, L. Del. (2020). A two-layer predictive emergency steering and escape assistant. *2020 American Control Conference (ACC)*, *2020-July*, 4849–4855. https://doi.org/10.23919/ACC45564.2020.9147455

Bärgman, J., Boda, C.-N., & Dozza, M. (2017a). Counterfactual simulations applied to SHRP2 crashes: The effect of driver behavior models on safety benefit estimations of intelligent safety systems. *Accident Analysis & Prevention*, *102*, 165–180. https://doi.org/https://doi.org/10.1016/j.aap.2017.03.003

Bärgman, J., Boda, C. N., & Dozza, M. (2017b). Counterfactual simulations applied to SHRP2 crashes: The effect of driver behavior models on safety benefit estimations of intelligent safety systems. *Accident Analysis and Prevention*, *102*, 165–180. https://doi.org/10.1016/j.aap.2017.03.003

Bella, F., & Silvestri, M. (2017). Interaction driver–bicyclist on rural roads: Effects of cross-sections and road geometric elements. *Accident Analysis and Prevention*. https://doi.org/10.1016/j.aap.2017.03.008

Bianchi Piccinini, G. F., Moretto, C., Zhou, H., & Itoh, M. (2018). Influence of oncoming traffic on drivers' overtaking of cyclists. *Transportation Research Part F: Traffic Psychology and Behaviour*, *59*, 378–388. https://doi.org/10.1016/j.trf.2018.09.009

Brännström, M., Coelingh, E., & Sjöberg, J. (2014). Decision-making on when to brake and when to steer to avoid a collision. *International Journal of Vehicle Safety*, *7*(1), 87. https://doi.org/10.1504/IJVS.2014.058243

Brännström, M., Sandblom, F., & Hammarstrand, L. (2013). A probabilistic framework for decision-making in collision avoidance systems. *IEEE Transactions on Intelligent Transportation Systems*, *14*(2), 637–648. https://doi.org/10.1109/TITS.2012.2227474

Bürkner, P.-C., & Vuorre, M. (2019). Ordinal Regression Models in Psychology: A Tutorial. *Advances in Methods and Practices in Psychological Science*, *2*(1), 77–101. https://doi.org/10.1177/2515245918823199

Cars, V. (n.d.). *City Safety with Steering Assist*. City Safety w/ Steering Assist (custhelp.com)

Chen, B.-C., Shih, C.-W., & Lin, Y. (2014). *Design of Forward Collision Warning System using Estimated Relative Acceleration and Velocity Vector*. SAE International. https://doi.org/https://doi.org/10.4271/2014-01-2030

Chen, M., Zhan, X., Zhang, X., & Pan, W. (2019). Localisation-based autonomous vehicle rear-end collision avoidance by emergency steering. *IET Intelligent Transport Systems*, *13*(7), 1078–1087. https://doi.org/10.1049/iet-its.2018.5348

Cicchino, J. B. (2017). Effectiveness of forward collision warning and autonomous emergency braking systems in reducing front-to-rear crash rates. *Accident Analysis*

and Prevention, *99*, 142–152. https://doi.org/10.1016/j.aap.2016.11.009
Clarke, D. D., Ward, P. J., & Jones, J. (1999). Processes and countermeasures in overtaking road accidents. *Ergonomics*, *42*(6), 846–867, https://doi.org/10.1080/001401399185333.
Dahl, J., Rodrigues de Campos, G., Olsson, C., & Fredriksson, J. (2018). Collision Avoidance: A Literature Review on Threat-Assessment Techniques. *IEEE Transactions on Intelligent Vehicles*, *PP*(c), 1–1. https://doi.org/10.1109/tiv.2018.2886682
Debnath, A. K., Haworth, N., Schramm, A., Heesch, K. C., & Somoray, K. (2018). Factors influencing noncompliance with bicycle passing distance laws. *Accident Analysis & Prevention*, *115*, 137–142. https://doi.org/10.1016/J.AAP.2018.03.016
Dozza, M., Schindler, R., Bianchi-Piccinini, G., & Karlsson, J. (2016). How do drivers overtake cyclists? *Accident Analysis and Prevention*. https://doi.org/10.1016/j.aap.2015.12.008
Euro NCAP (2020). "Test Protocol - AEB VRU systems"
Fildes, B., Keall, M., Bos, N., Lie, A., Page, Y., Pastor, C., Pennisi, L., Rizzi, M., Thomas, P., & Tingvall, C. (2015). Effectiveness of low speed autonomous emergency braking in real-world rear-end crashes. *Accident Analysis and Prevention*, *81*, 24–29. https://doi.org/10.1016/j.aap.2015.03.029
Ford. (n.d.). *Evasive Steering Assist*. https://www.ford.com/technology/driver-assist-technology/evasive-steering-assist/
Fredriksson R., F. K. (2014). Fredriksson R., Fredriksson K., & Strandroth J. (2014). Pre-crash motion and conditions of bicyclist-to-car crashes in Sweden. *International Cyclist Safety Conference 2014.*
Gibson, J. J., & Crooks, L. E. (1938). A Theoretical Field-Analysis of Automobile-Driving. *The American Journal of Psychology*, *51*(3), 453–471.
Gromke, C., & Ruck, B. (2021). Passenger car-induced lateral aerodynamic loads on cyclists during overtaking. *Journal of Wind Engineering and Industrial Aerodynamics*, *209*(August 2020), 104489. https://doi.org/10.1016/j.jweia.2020.104489
He, X., Liu, Y. Y. Y., Lv, C., Ji, X., & Liu, Y. Y. Y. (2019). Emergency steering control of autonomous vehicle for collision avoidance and stabilisation. *Vehicle System Dynamics*, *57*(8), 1163–1187. https://doi.org/10.1080/00423114.2018.1537494
Heesen, M. (2014). Interaction design of automatic steering for collision avoidance: challenges and potentials of driver decoupling.
Hillenbrand, J., Spieker, A. M., & Kroschel, K. (2006). A multilevel collision mitigation approach - Its situation assessment, decision making, and performance tradeoffs. *IEEE Transactions on Intelligent Transportation Systems*, *7*(4), 528–540. https://doi.org/10.1109/TITS.2006.883115
Hong, T., Kwon, J., Park, K., Lee, K., Hwang, T., & Chung, T. (2013). Development of a driver's intention determining algorithm for a steering system based collision avoidance system. *SAE Technical Papers*, *1*. https://doi.org/10.4271/2013-01-0054
Jafari, R., Zeng, S., Moshchuk, N., & Litkouhi, B. (2017). Reactive path planning for emergency steering maneuvers on highway roads. *Proceedings of the American Control Conference*, *1*, 2943–2949. https://doi.org/10.23919/ACC.2017.7963398

Keller, M., Hass, C., Seewald, A., & Bertram, T. (2014). Driving simulator study on an emergency steering assist. *Conference Proceedings - IEEE International Conference on Systems, Man and Cybernetics*, *2014-Janua*(January), 3008–3013. https://doi.org/10.1109/smc.2014.6974388

Kovaceva, J., Bálint, A., Schindler, R., & Schneider, A. (2020). Safety benefit assessment of autonomous emergency braking and steering systems for the protection of cyclists and pedestrians based on a combination of computer simulation and real-world test results. *Accident Analysis and Prevention*, *136*(October 2019), 105352. https://doi.org/10.1016/j.aap.2019.105352

Kovaceva, J., Nero, G., Bärgman, J., & Dozza, M. (2019). Drivers overtaking cyclists in the real-world: Evidence from a naturalistic driving study. *Safety Science*, *119*, 199–206. https://doi.org/10.1016/J.SSCI.2018.08.022

Kowshik, H., Caveney, D., & Kumar, P. R. (2011). Provable systemwide safety in intelligent intersections. *IEEE Transactions on Vehicular Technology*, *60*(3), 804–818. https://doi.org/10.1109/TVT.2011.2107584

Lamb, J. S., Walker, G. H., Fisher, V., Hulme, A., Salmon, P. M., & Stanton, N. A. (2020). Should we pass on minimum passing distance laws for cyclists? Comparing a tactical enforcement option and minimum passing distance laws using signal detection theory. *Transportation Research Part F: Traffic Psychology and Behaviour*, *70*, 275–289. https://doi.org/10.1016/j.trf.2020.03.011

Lexus. (n.d.).

Liers, H., & Hannawals, L. (2011). Benefit estimation of secondary safety measures in real-world pedestrian accidents. *In: 22nd International Enhanced Safety of Vehicles (ESV) Conference.*

Washington, D.C.

Ljung Aust, M, & Engström, J. (2011). A conceptual framework for requirement specification and evaluation of active safety functions. *Theoretical Issues in Ergonomics Science*, *12*(1), 44–65. https://doi.org/10.1080/14639220903470213

Ljung Aust, Mikael, & Dombrovski, S. (2013). Understanding and Improving Driver Compliance With Safety System. *The 23th International Technical Conference on the Enhanced Safety of Vehicles (ESV)*.

Llorca, C., Angel-Domenech, A., Agustin-Gomez, F., & Garcia, A. (2017). Motor vehicles overtaking cyclists on two-lane rural roads: Analysis on speed and lateral clearance. *Safety Science*, *92*, 302–310. https://doi.org/10.1016/J.SSCI.2015.11.005

Loos, S. M., Platzer, A., & Nistor, L. (2011). Adaptive cruise control: Hybrid, distributed, and now formally verified. *Lecture Notes in Computer Science (Including Subseries Lecture Notes in Artificial Intelligence and Lecture Notes in Bioinformatics)*, *6664 LNCS*, 42–56. https://doi.org/10.1007/978-3-642-21437-0_6

López, G., Pérez-Zuriaga, A. M., Moll, S., & García, A. (2020). Analysis of Overtaking Maneuvers to Cycling Groups on Two-Lane Rural Roads using Objective and Subjective Risk. *Transportation Research Record: Journal of the Transportation Research Board*, *2674*(7), 148–160. https://doi.org/10.1177/0361198120921169

Lübbe, N. (2015). *Integrated Pedestrian Safety Assessment: A Method to Evaluate Combinations of Active and Passive Safety*. http://publications.lib.chalmers.se/publication/225504-integrated-pedestrian-safety-

assessment-a-method-to-evaluate-combinations-of-active-and-passive-safe
Markkula, G., Boer, E., Romano, R., & Merat, N. (2018). Sustained sensorimotor control as intermittent decisions about prediction errors: computational framework and application to ground vehicle steering. *Biological Cybernetics*, *112*(3), 181–207. https://doi.org/10.1007/s00422-017-0743-9
Masayuki Shimizu;, Usami;, M., & Fujinami, H. (2008). *Development of Collision-Avoidance Assist System Operating at Driver Steering*. *39*(4), 41–46. https://doi.org/10.11351/jsaeronbun.39.4_41
Michon, J. A. (1985). A Critical View of Driver Behavior Models: What Do We Know, What Should We Do? In L. Evans & R. C. Schwing (Eds.), *Human Behavior and Traffic Safety* (pp. 485–524). Springer US. https://doi.org/10.1007/978-1-4613-2173-6_19
Moll, S., López, G., Rasch, A., Dozza, M., & García, A. (2021). Modelling duration of car-bicycles overtaking manoeuvres on two-lane rural roads using naturalistic data. *Accident Analysis and Prevention*, *160*(May). https://doi.org/10.1016/j.aap.2021.106317
Nosratinia, M., Lind, H., Carlsson, S., & Mellegård, N. (2010). A holistic decision-making framework for integrated safety. *IEEE Intelligent Vehicles Symposium, Proceedings*, 1028–1035. https://doi.org/10.1109/IVS.2010.5547975
Polychronopoulos, A., Tsogas, M., Amditis, A., Scheunert, U., Andreone, L., & Tango, F. (2004). Dynamic situation and threat assessment for collision warning systems: The EUCLIDE approach. *IEEE Intelligent Vehicles Symposium, Proceedings*, 636–641. https://doi.org/10.1109/ivs.2004.1336458
Rasch, A., Boda, C.-N., Thalya, P., Aderum, T., Knauss, A., & Dozza, M. (2020). How do oncoming traffic and cyclist lane position influence cyclist overtaking by drivers? *Accident Analysis & Prevention*, *142*(July 2020). https://doi.org/https://doi.org/10.1016/j.aap.2020.105569
Rasch, A., Moll, S., López, G., García, A., & Dozza, M. (2022). Drivers' and cyclists' safety perceptions in overtaking maneuvers. *Transportation Research Part F: Traffic Psychology and Behaviour*, *84*(September 2021), 165–176. https://doi.org/10.1016/j.trf.2021.11.014
Rasch, A., Dozza, M. (2023). The effect of speed on driver behavior when overtaking cyclists: Results from driving-simulator and test-track data. *ICTCT 2023 conference.* Catania, Italy. https://www.ictct.net/wp-content/uploads/35-Catania-2023/ICTCT_Catania_2023_abstract_20.pdf.
Rasch, A. (2023). Drivers overtaking cyclists and pedestrians: Modeling road-user behavior for traffic safety. PhD thesis. Chalmers University of Technology. *https://research.chalmers.se/publication/534378/file/534378_Fulltext.pdf.*
Rasch, A., Tarakanov, Y., Tellwe, G., & Dozza, M. (in press). Drivers passing cyclists: How does sight distance affect safety? Results from a naturalistic study. *Journal of Safety Research.*
Rosén, E. (2013). Autonomous Emergency Braking for Vulnerable Road Users. *Proceedings of IRCOBI Conference*, 618–627. http://www.ircobi.org/wordpress/downloads/irc13/pdf_files/71.pdf
Rubie, E., Haworth, N., Twisk, D., & Yamamoto, N. (2020). Influences on lateral passing

distance when motor vehicles overtake bicycles: a systematic literature review. *Transport Reviews*, *40*(6), 754–773. https://doi.org/10.1080/01441647.2020.1768174

Sander, U. (2017). Opportunities and limitations for intersection collision intervention—A study of real world 'left turn across path' accidents. *Accident Analysis and Prevention*, *99*, 342–355. https://doi.org/10.1016/j.aap.2016.12.011

Sander, U. (2018). *Predicting Safety Benefits of Automated Emergency Braking at Intersections Virtual simulations based on real-world accident data*. https://research.chalmers.se/publication/504728/file/504728_Fulltext.pdf

Schwab, A. L., & Meijaard, J. P. (2013). A review on bicycle dynamics and rider control. *Vehicle System Dynamics*, *51*(7), 1059–1090. https://doi.org/10.1080/00423114.2013.793365

Seewald, A., Haß, C., Keller, M., & Bertram, T. (2015). Emergency Steering Assist for Collision Avoidance. *ATZ Worldwide*, *117*(1), 14–19. https://doi.org/10.1007/s38311-015-0147-1

Shackel, S. C., & Parkin, J. (2014). Influence of road markings, lane widths and driver behaviour on proximity and speed of vehicles overtaking cyclists. *Accident Analysis & Prevention*, *73*, 100–108. https://doi.org/10.1016/j.aap.2014.08.015

Singer, J. D., & Willett, J. B. (2003). *Applied Longitudinal Data Analysis*. Oxford University Press. https://doi.org/10.1093/acprof:oso/9780195152968.001.0001

Sjöberg, J., Coelingh, E., Ali, M., Brännström, M., Falcone, P., Assjobergchalmersse, J. O., Www, W. E. B., & Se, C. (2010). DRIVER MODELS TO INCREASE THE POTENTIAL OF AUTOMOTIVE ACTIVE SAFETY FUNCTIONS. *18th European Signal Processing Conference (EUSIPCO-2010)*, 204–208.

Summala, H. (2007). Towards Understanding Motivational and Emotional Factors in Driver Behaviour: Comfort Through Satisficing. In P. C. Cacciabue (Ed.), *Modelling Driver Behaviour in Automotive Environments: Critical Issues in Driver Interactions with Intelligent Transport Systems* (pp. 189–207). Springer London. https://doi.org/10.1007/978-1-84628-618-6_11

Uittenbogaard, J., Rodarius, C., & Camp, O. M. G. C. (2016). *CATS Deliverable 1.2: CATS car-to-cyclist accident scenarios*. Helmond: TNO.

UNECE. (2021). *R79*.

Vassilis, P., Dimitris, N., Evangelia, P., & Nicolas, M. (2015). The effects of changes in the traffic scene during overtaking. *Accident Analysis & Prevention*, *79*, 126–132, https://doi.org/10.1016/j.aap.2015.02.025

Yoshimura, M., Fujimoto, G., Kaushik, A., Kumar, B., Matthew, P., Sood, I., Sarkar, K., Muneer, A., More, A., Tsuchiya, M., Araki, S., Hebber, A., Tieleman, T., & Yasui, Y. (2020). *Autonomous Emergency Steering Using Deep Reinforcement Learning For Advanced Driver Assistance System*. *2*.